

DNA MEDIATED SELF ASSEMBLY OF CARBON NANOTUBES INTO
NANORINGS

by
Ali Yasin Sonay

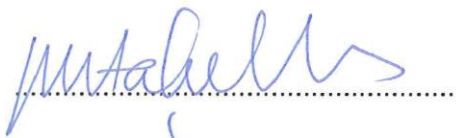
Submitted to the Institute of Graduate Studies in
Science and Engineering in partial fulfillment of
the requirements for the degree of
Master of Science
in
Biotechnology

Yeditepe University
2011

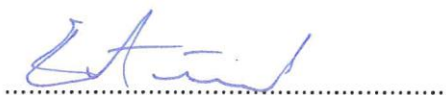
DNA MEDIATED SELF ASSEMBLY OF CARBON NANOTUBES INTO
NANORINGS

APPROVED BY:

Prof. Mustafa Culha
(Thesis Supervisor)

A handwritten signature in blue ink, appearing to read 'Mustafa Culha', written over a horizontal dotted line.

Prof. Ertugrul Kilic

A handwritten signature in blue ink, appearing to read 'Ertugrul Kilic', written over a horizontal dotted line.

Assist. Prof. Andrew Harvey

A handwritten signature in blue ink, appearing to read 'A. Harvey', written over a horizontal dotted line.

DATE OF APPROVAL: / /

ACKNOWLEDGEMENTS

I would like to thank my advisor, Prof. Mustafa Culha, for his support at every point on my Masters education, for providing me the atmosphere to flourish and build my confidence. He showed me how an advisor should approach and guide his students.

I also want to thank Yeditepe University Nanobiotechnology Group Members that supported me during my thesis. I am grateful to Seda Keleştemur, Sevcan Öztürk and Şaban Kalay for providing me the chemicals that made this thesis possible as well as their stimulating discussions. I thank Mine Altunbek for her help on my thesis. I am also grateful to Kemal Keseroğlu, İsmail Sayın and İlkur Sur for their support, knowledge and advises that helped me immensely during my Masters education. I am grateful to my friends Ahmet Burak Çağlayan, Esen Efeoğlu, Gökcan Şahin, Sercan Keskin, Ertuğ Avcı, who were with me during past years that made hard work days bearable and entertaining.

I also want to thank Prof. Ertugrul Kilic and Assist. Prof. Andrew Harvey for their help with my thesis. I want to express my gratitude to TUBİTAK and Yeditepe University for the financial support during my master education (Project No: 108T605).

I am grateful to my family who did all they can to prepare me for this life and showed me the way to become a better person.

I am eternally grateful to Tuğçe Bilgin for showing me how to face the challenges of life and remain strong for the sake of your loved ones. Without her help and support, I wouldn't be able to finish this thesis.

This thesis is dedicated to those who strive to create meaningful stories from their lives by being compassionate, kind and curious. Their tireless search for beauty and truth makes this world worth living.

ABSTRACT

DNA MEDIATED SELF ASSEMBLY OF CARBON NANOTUBES INTO NANORINGS

Carbon Nanotubes(CNT) are newly discovered nanomaterials that are the focus of intense research because of their physical, chemical, electrical and optical characteristics that extend beyond other materials. Due to these properties, they have a variety of applications in different areas like nanoelectronics, tissue engineering, biosensor technologies and drug delivery. However, the main problem with the use of carbon nanotubes is their highly hydrophobic nature. Due to their strong affinity towards each other to form aggregates, it becomes difficult to extend their use into a wide range of applications.

DNA attracts the attention of researchers with its ability to disperse nanotubes similar to a surfactant. DNA-CNT interaction involves two different approaches. One of them is a non-covalent approach where DNA bases are adsorbed to CNT walls and DNA wraps around the Carbon Nanotubes. This approach protects the intrinsic properties of the carbon nanotubes but offer limited potential for self-assembly research. On the other hand, covalent DNA binding to CNTs allows the use of DNA hybridization properties and has the potential to produce complex shapes. In this work, Single Walled Carbon Nanotubes (SWCNTs) were functionalized with carboxyl acid groups and oligodeoxynucleotides(ODNs) were covalently bound to them via ODNs' amine terminated end. By changing the concentration of ODN linker molecules that binds two different ODN bound SWCNTs, nanoring structures are formed. Also the factors affecting the formation of these structures are addressed as well as their behaviour under extreme heat and sonication. These nanoring structures and the factors affecting them were studied under Atomic Force Microscopy(AFM). The knowledge obtained from this work shows the preparation of nanorings by using DNA mediated self-assembly of SWCNTs, which can be used for designing more complex structures and can be applied for photothermal therapy, nanoelectronics, drug and gene delivery.

ÖZET

KARBON NANOTÜPLERİN DNA İLE KENDİLİĞİNDEN DÜZENLENME YÖNTEMİYLE NANOHALKA YAPILAR OLUŞTURMASI

Karbon Nanotüpler diğer malzemelerden üstün fiziksel, kimyasal, elektriksel ve optik özellikleri nedeniyle yoğun araştırmaların odağında olan yeni keşfedilmiş nanomalzemelerdir. Bu özellikleri nedeniyle nanoelektronik, doku mühendisliği biyosensör teknolojileri ve ilaç taşıma sistemleri gibi farklı alanlarda birçok uygulamaya sahiptir. Buna rağmen Karbon Nanotüp kullanımıyla ilgili temel sorun onların hidrofobik yapıda olması ve kendilerine olan çekimleri nedeniyle yığıntılar oluşturmasıdır ve bu durum, bu alanlardaki geniş çaplı uygulamaları engellemektedir.

DNA, nanotüpleri surfaktantlar gibi çözüme özelliğiyle araştırmacıların ilgisini çekmektedir. DNA-KNT etkileşimleri iki farklı yöntemden oluşur. Bunlardan biri olan kovalent olmayan yöntemde DNA bazıları KNT'ün duvarına tutunur ve DNA Karbon Nanotüp'ün etrafına sarılır. Bu yöntem karbon nanotüplerin kendine has özelliklerini korumakla birlikte kendiliğinden düzenlenme araştırmaları için sınırlı potansiyele sahiptir. Diğer taraftan, KNT'lere kovalent DNA bağlanması DNA'nın hibridizasyon özelliklerinin kullanılmasını sağlar ve karmaşık yapıların oluşturulmasına imkan verir. Bu çalışmada Tek Katmanlı Karbon Nanotüpler(TKKNT) karboksil asit grupları ile fonksiyonellenmiş ve oligodeoksinukleotidlere(ODN) amin grubuyla biten uçlarından kovalent olarak bağlanmışlardır. ODN bağlı iki farklı TKKNT'ü birbirine bağlayan DNA ara molekülünün konsantrasyonunu değiştirerek nanohalka yapıları oluşturulmuştur. Aynı zamanda bu yapıların oluşmasını etkileyen faktörler, aşırı sıcaklık ve sonikasyon uygulandığındaki davranışları belirlenmiştir. Bu nanohalka yapıları ve onları etkileyen faktörler Atomik Güç Mikroskobu(AFM) kullanılarak araştırılmıştır. Bu çalışmadan elde edilen bilgi DNA ile kendiliğinden düzenlenme metodu kullanılarak TKKNT'lerden daha kompleks yapıların oluşmasında, fototermal terapi, nanoelektronik, gen ve ilaç taşıma sistemleri için kullanılacak nanohalka oluşturulmasını göstermektedir.

TABLE OF CONTENTS

ABSTRACT	iv
ÖZET	v
LIST OF FIGURES	vii
LIST OF TABLES	xi
LIST OF SYMBOLS / ABBREVIATIONS.....	xii
1. INTRODUCTION	1
2. THEORETICAL BACKGROUND.....	6
2.1. CARBON NANOTUBES	6
2.1.1. Chemical Modifications of Carbon Nanotubes	7
2.1.2. Applications of Carbon Nanotubes	8
2.2. ASSEMBLY: TOP-DOWN AND BOTTOM-UP APPROACHES	10
2.2.1. Top-Down Approaches	10
2.2.2. Bottom-Up Approaches	12
2.2.2.1. Self-Assembly from a Drying Droplet.....	13
2.2.2.2. Template-Assisted Self-Assembly.....	14
2.2.2.3. Programmed Self-Assembly	15
3. MATERIALS.....	18
3.1. REAGENTS.....	18
3.2. OLIGONUCLEOTIDES.....	18
4. MATERIALS.....	20
4.1. CARBOXYLIC ACID FUNCTIONALIZATION OF CARBON	
NANOTUBES	20
4.2. CHEMICAL ATTACHMENT OF AMINE TERMINATED.....	
OLIGONUCLEOTIDES TO SINGLE WALLED	
CARBON NANOTUBE.....	21
4.3. CONSTRUCTION OF NANOSTRUCTURES.....	22
4.3.1. Raman Instrumentation.....	23
4.3.2. FTIR Analysis	23
4.3.3. Scanning Electron Microscopy Analysis	23

4.3.4. Atomic Force Microscopy Analysis	23
5. RESULTS AND DISCUSSION	24
5.1. CHARACTERIZATION OF OLIGONUCLEOTIDE BINDING TO	
SINGLE WALLED CARBON NANOTUBES.....	24
5.2. CONSTRUCTING NANORINGS USING ODN LINKERS	25
5.2.1. Constructing Nanorings with ODNs D1 and D2	25
5.2.2. Effect of ODN Linker Concentration on Nanorings	34
5.2.3. Effect of ODN Linker Length on Nanorings	36
5.2.4. Constructing Nanorings with ODNs D3 and D4	38
5.2.5. Effect of Sonication and Heat on the Stability of Nanorings.....	40
6. CONCLUSION AND RECOMMENDATIONS	43
6.1. CONCLUSION.....	43
6.2. RECOMMENDATIONS	44
7. REFERENCES	46

LIST OF FIGURES

Figure 1.1. Size comparison of the structures from micro to nano	1
Figure 1.2. 16th century Iranian Crucible forged Damascus steel sword	2
Figure 1.3. Examples of top-down approach constructed mills made of silicon..... using lithographic techniques and bottom-up approach-self assembled..... DNA scaffold	4
Figure 1.4. Various application areas of different nanoparticles	5
Figure 2.1. Representative diagrams of SWCNT and MWCNT	7
Figure 2.2. DNA wrapping of Carbon Nanotubes and covalently bound DNA on..... Carbon Nanotubes	8
Figure 2.3. Applications of Carbon Nanotubes as AFM Probe tips, substrates for..... neuronal growth and Carbon Nanotube test tubes	9
Figure 2.4. Schematic representation of photolithography and CNT arrays using photolithography	11
Figure 2.5. Ultrathin CNT film at water hexane interface(A) and SEM image of..... CNT film assembled at water hexane interface	12
Figure 2.6. Image of drying pattern of CNT-F68 suspension where CNTs are concentrated at the center of the droplet	14

Figure 2.7. Representation of MEH-PPV concentric rings and CNT deposition on..... the surface and optical image of the formed surface after MEH-PPV is removed.....	14
Figure 2.8. Nanostructures created based on DNA mediated self-assembly.....	17
Figure 4.1. Raman spectra of pristine SWCNT and carboxylated SWCNT	20
Figure 4.2. FTIR spectra of pristine SWCNTs and carboxyl functionalized	21
SWCNTs	21
Figure 4.3. DNA functionalization of SWCNTs in the presence of EDC.....	22
Figure 5.1. Raman spectra of ODN bound SWCNTs	24
Figure 5.2. FTIR spectra of ODN bound SWCNTs	25
Figure 5.3. Representation of hybridization of ODNs D1 and D2 with D7	26
Figure 5.4. Proposed DNA mediated nanoring model (not in scale)	26
Figure 5.5. Carbon nanoring structures formed with ODNs D1 and D2 and ODN	27
linker D7 on glass surfaces.....	27
Figure 5.6. Carbon nanoring structures formed with ODNs D1 and D2 on mica	28
Figure 5.7. Schematic presentation of drying pattern of SWCNT samples.....	29
Figure 5.8. AFM image of 4-6 nm high carbon nanorings between contact line and	30
highly concentrated region	30
Figure 5.9. Close up AFM image of 4-6 nm high carbon nanorings between	30
contact line and highly concentrated region.....	30

Figure 5.10. AFM image of 10-12 nm high carbon nanorings closer to highly concentrated region.....	31
Figure 5.11. AFM image of 10-12 nm high carbon nanorings closer to highly concentrated region.....	31
Figure 5.12. Close up AFM image of 10-12 nm high carbon nanorings closer to highly concentrated region.....	32
Figure 5.13. AFM image of combination of two nanorings indicated in red line analysis	33
Figure 5.14. AFM image of nanoring structure composed of long SWCNTs.....	33
Figure 5.15. AFM image of incomplete nanorings and aggregates.....	34
Figure 5.16. Closer AFM image of incomplete nanorings and aggregates	35
Figure 5.17. AFM image of incomplete nanorings and aggregates formed by 2,5 mM ODN linker and deformed nanorings due to incomplete aggregation formed by 10 mM ODN linker	36
Figure 5.18. Representation of hybridization of ODNs D1 and D2 with ODN linkers D5 and D6	37
Figure 5.19. AFM image of round shaped aggregates formed by D5 ODN linker and D6 ODN linker	38
Figure 5.20. Representation of hybridization of ODNs D3 and D4 with ODN linker D8	38
Figure 5.21. Non-shaped SWCNT aggregates formed by ODNs D3 and D4 with a general image and a close up	39

Figure 5.22. Opening up of nanorings after sonication 40

Figure 5.23. SEM image of aggregates composed of bundles and rope like.....
structures formed after heating of nanorings and a close up image of
the same structure..... 41

LIST OF TABLES

Table 3.1. The sequences of ODNs used for constructing nanorings	19
--	----

LIST OF SYMBOLS / ABBREVIATIONS

1D	One dimensional
AFM	Atomic Force Microscopy
AgNP	Silver nanoparticle
AuNP	Gold nanoparticle
CNT	Carbon nanotube
d.nm	diameter in nanometer scale
DNA	Deoxyribonucleic acid
dsDNA	Double-stranded deoxyribonucleic acid
EDC	1-ethyl-3-(3-dimethylaminopropyl) carbodiimide
e-beam	Electron-beam
FTIR	Fourier Transform Infra Red
Hz	Hertz
kDa	kilo Dalton
kV	kilo Volt
min	minute
MWCNT	Multi Walled Carbon Nanotube
MNP	Magnetic nanoparticle
MRI	Magnetic resonance imaging
nm	nanometer
NP	Nanoparticle
NASA	National Aeronautics and Space Administration
ODN	Oligodeoxyribonucleic acid
QD	Quantum dot
RNA	Ribonucleic acid
SWCNT	Single Walled Carbon Nanotube
SEM	Scanning Electron Microscopy
TEM	Transmission Electron Microscopy

1. INTRODUCTION

Nanotechnology is derived from the word Nano, which means dwarf in Greek. This word points to the operating size of nanotechnology, which is 10^{-9} m. While needles used in medical delivery chips are $100\ \mu\text{m}$, a red blood cell is between $2\text{-}5\ \mu\text{m}$. A double stranded DNA is about $2\ \text{nm}$ wide and its 10 base pairs are $3.4\ \text{nm}$ long, which is equivalent to a complete turn of helix structure. Gold nanoparticles, which may vary in size can be between $100\ \text{nm}$ and down to $3\ \text{nm}$ depending on the synthesis techniques.

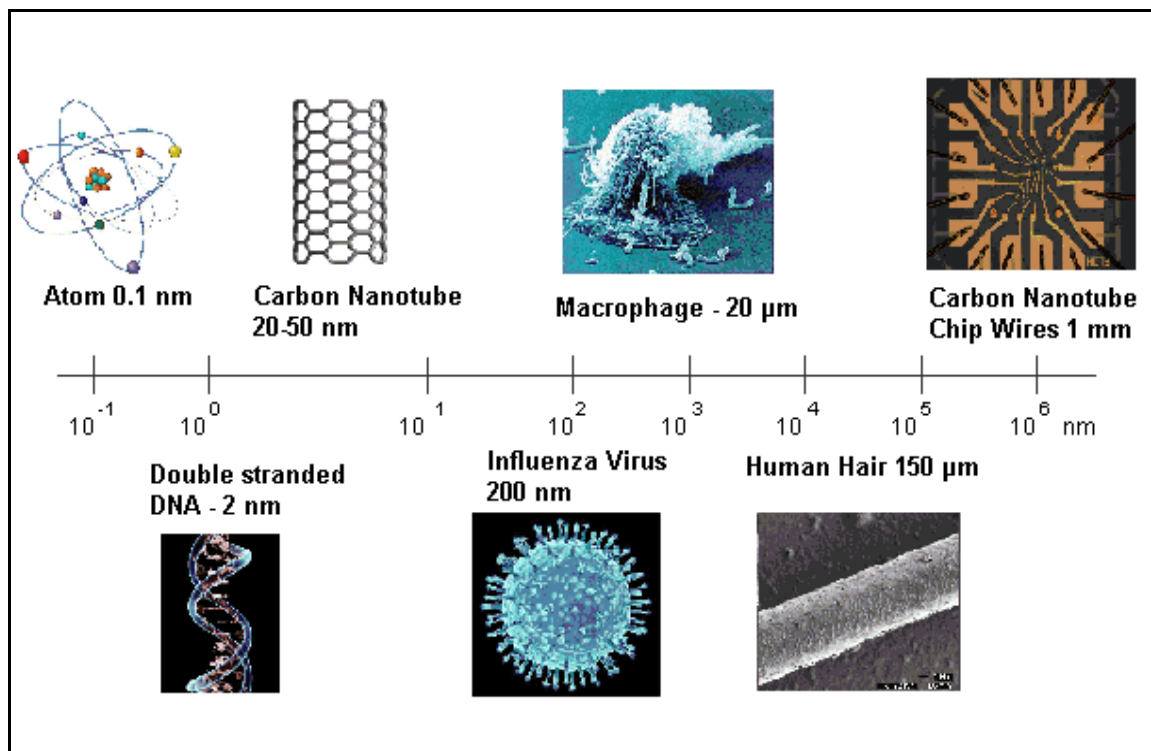


Figure 1.1. Size comparison of structures from micro to nanometers

Eventhough the concept is relatively new, the use of nanotechnology dates back further. For example Damascus Steel, a type of steel that is used in the Syrian region against Crusaders, is known for its resilience, extreme sharpness and flexibility and also contains distinctive band patterns. Recent research conducted using high resolution electron microscopy showed that Damascus steel contains cementite nanowires and carbon nanotubes [1].

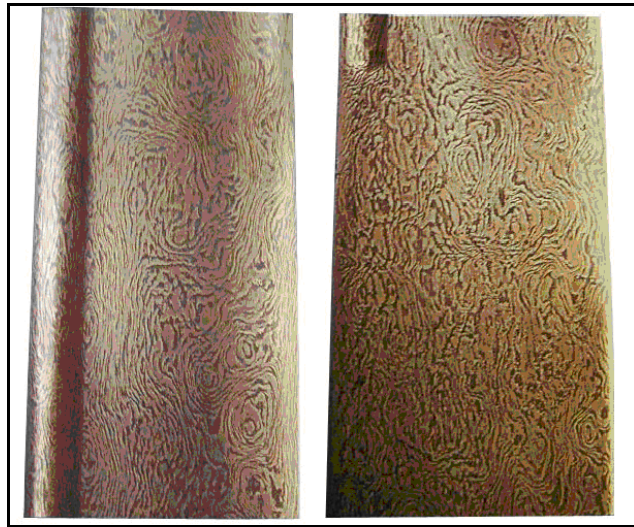


Figure 1.2. 16th century Iranian crucible forged Damascus steel sword [1]

Modern nanotechnology is generally accepted to be conceptualized and inspired by Richard Feynman in his talk “There’s plenty of room at the bottom” given to the American Physical Society in 1959 where he suggested direct manipulation of atoms provides a lot of opportunities where ordinary laws of matter like gravity have little importance and surface tension, Van der Waals attraction would have more importance [2]. Yet, the term Nanotechnology is first used by a Japanese scientist Norio Taniguchi of the Tokyo University of Science in a talk in 1974 where he defined nanotechnology as “production technology to get extra high accuracy and ultra fine dimensions, i.e. the preciseness and fineness on the order of 1 nm (nanometer), 10^{-9} meter in length” [3]. However, molecular nanotechnology, a term that describes a nanoscale assembler able to replicate itself and perform autonomous functions is also described by Eric Drexler [4]. Nowadays, the accepted definition of nanotechnology is “The creation of functional materials, devices and systems through control of matter on the nanometer length scale (1-100 nanometers), and exploitation of novel phenomena and properties (physical, chemical, biological, mechanical, electrical...) at that length scale” according to NASA [5]. As Feynman predicted, laws of gravity and other Newtonian concepts are insignificant when dealing with materials in nanoscale. It is observed that such nanoparticles do not behave according to Newtonian mechanics but according to Quantum mechanics. Schrodinger’s equation provides explanation of these interactions and behaviour since it possesses an understanding of the property of atoms. Any process or structure composed of atoms are described with

this equation [6]. While Feynman's lecture was provocative and inspiring, experimental nanotechnology lagged behind his visions since there weren't any equipment to accomplish what he proposed. Later, with the invention of Scanning Microscopy in 1981 [7], the manipulation and observation of atoms became possible. Chemistry also caught up with the nanotechnology with producing unique nanomaterials with special electronic, optical and chemical properties like Quantum dots and Carbon Nanotubes.

Nanotechnology contains several challenges that need to be overcome to better control nanoparticles and use them in electronics, optics and biomedical applications. Two main problems are synthesis of pure nanoparticles with desired shape and size and assembly of these nanoparticles into a desired pattern [8]. While chemists work on further purification and synthesis methods, assembly of nanoparticles attract attention of engineers, physicists and molecular biologists in addition to chemists because self-assembly can be achieved in various ways. Self-assembly methods can be divided into two main approaches: top-down and bottom-up. Top-down approaches involve the bulk material as a starting point and divide, carve or shape them into a desired pattern mainly using lithography techniques. These lithography can vary depending on the application, but the main lithography types are: extreme UV lithography [9], ion beam lithography [10], photolithography [11], X-ray lithography [12] and electron beam lithography [13]. The patterns and devices constructed with these methods can be applied to various areas like microfluidics [14], lab-on-a-chip applications [15] and can be used to aid analytical techniques like DNA [16], RNA [17], protein detection [18] as well as single cell analysis [19]. However these lithography methods require expensive equipment, facilities and trained personnel so they are not widely applicable [20]. On the other hand, bottom up approaches are less expensive, do not require extensive training or facilities, so they are preferred more. These approaches include the assembly of nanoscale materials and bring them together to form a desired shape or pattern both in suspension and on surfaces while lithographic applications are limited to surfaces. Bottom-up approaches utilize the chemical interaction between atoms and program nanoparticles to come together in a desired shape [21]. This process is called self-assembly because the nanoparticles themselves form this shape. To accomplish self-assembly, nanoparticles are programmed through functionalization and interaction between macromolecules. Examples include DNA [22] or peptide [23] directed self-assembly of nanoparticles where the macromolecules on nanoparticle direct it towards a specific shape

or pattern. Because of ease of use and manufacture as compared to lithography methods, self-assembly attracted the interest of many researchers.

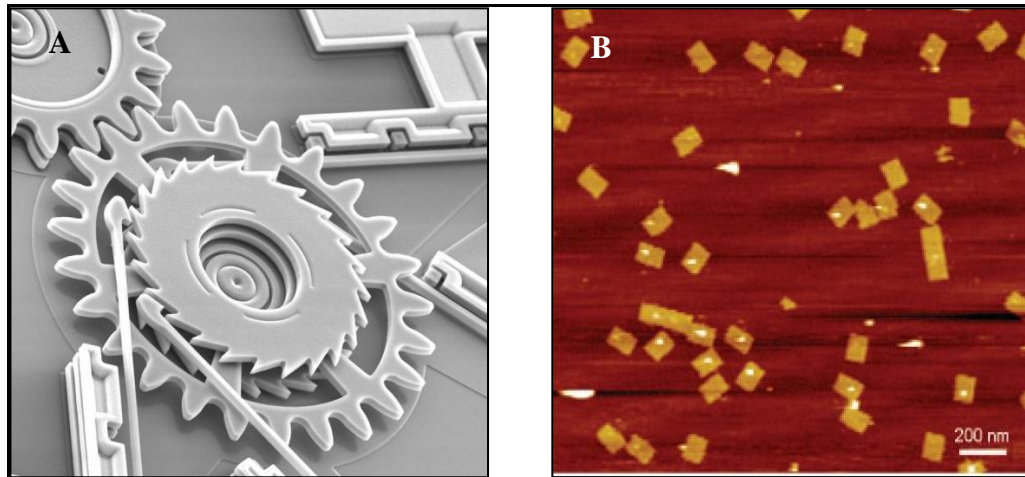


Figure 1.3. A. Examples of top-down approach-constructed mills made of silicon using lithographic techniques [24] and B. Bottom up approach-self assembled DNA nanoscaffold [25]

The main nanoparticles that are synthesized and used in nanotechnological research include gold nanoparticle (AuNP), silver nanoparticle (AgNP), magnetic nanoparticle (MNP), quantum dot (QD) and carbon nanotube (CNT). AuNP and AgNP is commonly denoted as noble metal nanoparticles and preferred for their unique optical and plasmonic properties [26] and used in techniques such as Surface Plasmon Resonance (SPR) [27] and Surface Enhanced Raman Scattering (SERS) [28]. Since AuNPs are biocompatible [29], stable and easily functionalized, most of the self-assembly research is conducted using AuNPs [30] and they are applied for photothermal therapy [31], gene and drug delivery [32]. AgNPs are used in many applications including commercial products due to their antibacterial [33] and wound healing properties [34]. MNPs, due to their easy functionalization and enhanced magnetic capacities used in newly developed isolation and purification technologies [35] and bioassays for rapid and highly sensitive detection [36] since they can be manipulated under magnetic fields. They are also used for MRI imaging technologies [37]. Quantum dots are semiconductor nanoparticles confined in a small space ranging between 1-10 nm [38] and have different fluorescence properties based on their size. Their confinement gives them a narrow emission and broad excitation

spectra [39]. They are considered as an alternative to fluorescent dyes because of their resistance to photobleaching [40]. CNTs are one of the most widely applied nanomaterials due to their high tensile strength [41], high aspect ratio [42], unique electrical [43] and physicochemical properties [44]. This makes them useful tools in chemistry, physics and biology. They can be used for nanoelectronics [45], AFM tips [46], drug delivery [47], photothermal therapy [48] and biosensor technologies [49]. One of the major obstacles in front of these technologies is efficient dispersion and organization of CNTs into defined patterns.

The aim of this study is to investigate DNA hybridization directed self-assembly of CNTs to forming nanoring structures. SWCNTs are chosen as a model in this study because of their flexibility and wide range of electronic properties that may have a variety of applications in biosensing, drug and gene delivery, and imaging as AFM tips. In this study SWCNTs are carboxyl functionalized and cross-linked with oligonucleotides (ODN), then using an ODN linker, these oligonucleotides are brought together in a nanoring formation. The structures are analyzed using Raman Spectroscopy, IR Spectroscopy, SEM and AFM.

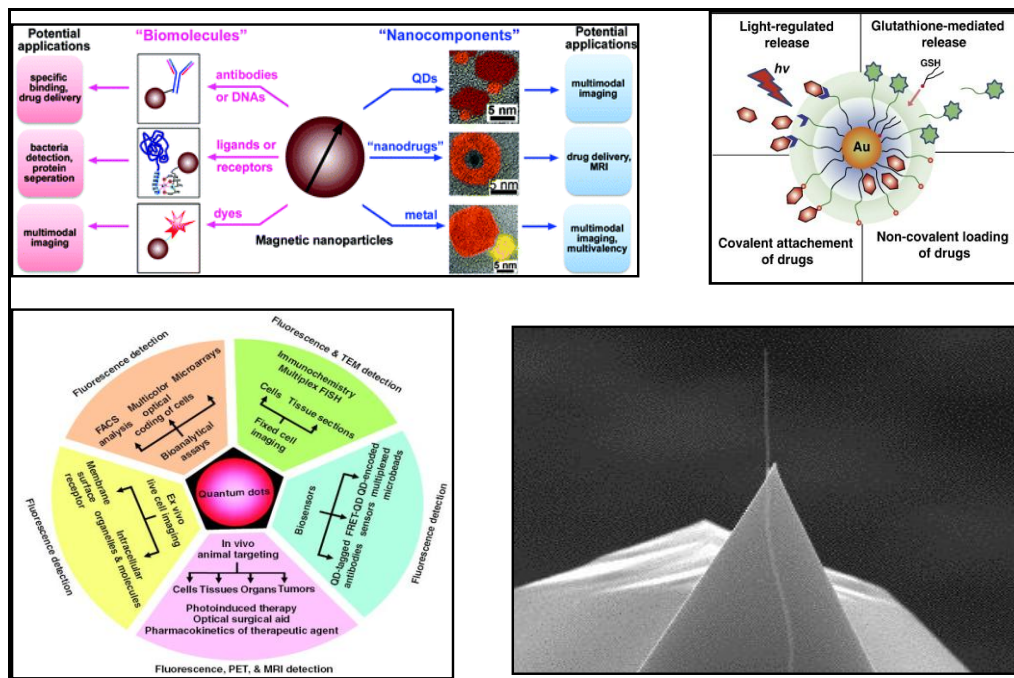


Figure 1.4. Various application areas of different nanoparticles [32, 36, 39, 46]

2. THEORETICAL BACKGROUND

This chapter first gives a background information about carbon nanotubes(CNTs) and their applications, then discusses the top down and bottom up approaches that are applied to CNTs with potential new technologies.

2.1. CARBON NANOTUBES

CNTs are hollow cylinder-shaped nanostructures, composed of carbon atoms. They can be considered as folded graphene sheets, first discovered by Iijima in 1991 [50]. From that point forward, they have been at the center of intense research in a variety of fields including electronics [51], biomedicine [52], physics [53], chemistry [54] and material science [55]. The excitement comes from their unique optical, electrical, chemical properties and high tensile strength and high aspect ratio [56]. They can occur in two types, Multi-walled Carbon Nanotubes(MWCNT) [57] and Single-Walled Carbon Nanotubes(SWCNT) [58]. MWCNTs are composed of several graphene sheets forming a tube around each other with a hollow core. Their size can range between 2-100 nm in width and their length can range from 1 μm to 10 μm [59]. SWCNTs are composed of only a single graphene layer, which makes them more flexible. Their thickness ranges between 0.4 to 2 nm [60]. CNTs are composed of hexagonal carbon structures held together by Van der Waals forces. CNTs are produced by electric arc [61], laser ablation [62], Chemical Vapor Deposition(CVD) [63] and gas phase catalytic processes(HiPco) [64]. Their growth occurs in the presence of metal catalysts, Fe, Co, Ni [65].

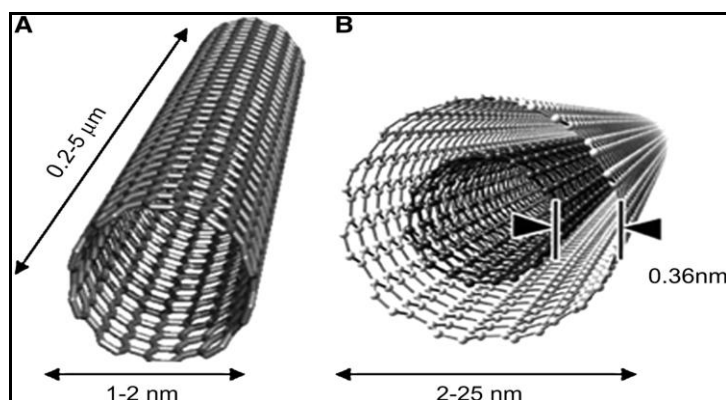


Figure 2.1. Representative Diagrams of A. SWCNT and B. MWCNT [66]

2.1.1. Chemical Modifications of Carbon Nanotubes

Because of intra-molecular Van der Waals bonds, CNTs tend to bundle and since their affinity is much higher than their affinity to water, they are hard to solubilize and disperse in water [67]. To use them more efficiently, there are various chemical modification routes that introduce new functional groups onto CNTs [68]. One of the most common chemical modification routes of CNTs is carboxylation with strong acids such as HNO_3 and H_2SO_4 under reflux [69]. Also SOCl_2 treatment also solubilizes CNTs in various organic solvents with additional functionalization of alkane groups where they become soluble in hexane [70]. For the modification of CNTs with biological macromolecules, amidation [71] and esterification [72] reactions are used to covalently bound macromolecules to CNT surfaces through the carboxyl group achieved with oxidation. CNTs interact with biological molecules such as DNA and proteins in two ways. The first one is non-covalent interactions that mostly depends on π - π stacking interaction where DNA [73] or proteins [74] adsorbed to the CNT surface. For example, sonicated CNTs are dispersed in water using DNA as a mediator wrapping around CNTs since it has hydrophobic bases and a hydrophilic backbone [75]. Advantages of this type of interaction include solubilizing CNTs without chemical damage, which may change electrical, optical and structural properties of CNTs [76]. However, the disadvantage of this method is weakness of the attachment and dissociation of biomolecule-CNT complexes [77]. For a permanent chemical bonding, CNTs are functionalized using acid treatment, which introduce new functional groups onto CNT surface. DNA [78] and proteins [79] can be covalently linked with functionalized CNTs via crosslinking agents and further chemical treatments. The

disadvantage of this process is to damage CNTs, which makes them less efficient for further applications [80].

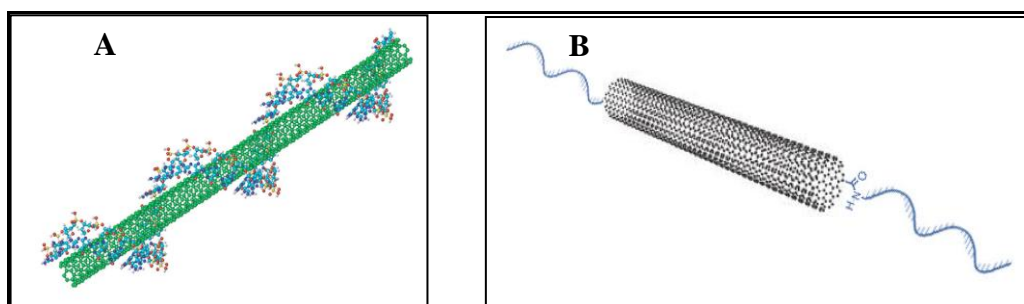


Figure 2.2. A. DNA wrapping around Carbon Nanotubes [73] and B. Covalently bound DNA on Carbon Nanotubes

2.1.2 Applications of Carbon Nanotubes

Today, there are many potential applications of CNTs in biomedicine, electronics, physics and material science due to their chemical and physical properties. This section covers some of the literature reports discussing possible uses of CNTs in the mentioned fields.

Carbon nanotubes are used as biosensors because of their small size and high surface area, thus making biosensors more sensitive [81]. Because of their high conductance of electricity, upon the binding of specific DNA, protein or small molecules, their conductance changes significantly, indicating the presence of the molecule in question [82]. Some examples include detection of Cytochrome C from adsorption [83], hydrogen peroxide detection [84] and Alkaline Phosphatase enzyme coupled DNA detection, which is highly sensitive with a detection limit of 1 pg L^{-1} [85].

Despite the claims that CNTs are toxic [86], others indicate that it is not the CNTs that are toxic, but rather the metal catalysts used for the growth of CNTs [87]. To test this, researchers used MWCNTs free from metal catalysts as bioscaffolds to mediate the growth and differentiation of neuronal cells and they have successfully grown neuronal cells on top of this bioscaffold [88]. With their biosensor capabilities, it is suggested that CNTs may be used for dual purposes, as scaffolds and as biosensors that modulate and

measure the intracellular changes during the signal transmission of neurons [89]. Due to their functionalization and membrane penetration abilities, CNTs are used to carry insoluble drugs, proteins and DNA, thus both carrying their cargo within the cells and preventing it from enzymatic degradation [90]. This has been demonstrated with different enzymes like Cytochrome C [91] and β -Lactate [92]. Another approach is the production of nano test tubes where CNTs contain a closed end and the chemical is placed inside of CNT [93]. Then, the open side is sealed with chemical modification, which may further develop into the production of nanopills. One of the most exciting use of CNTs is their applications as Scanning Probe tips [94] since they are ideal because of their small size and high electrical conductance. A conventional AFM tip is about 10 nm in thickness [95] whereas the thickness of SWCNTs is around 1-2 nm, which increases the resolution. Also their stiffness and flexibility make them suitable candidates for AFM tips. Use of AFM tips enable researchers to see the structure of proteins and DNA as well as emergence of new concepts like nanosurgery where AFM tips are used to remove aberrations from cellular structures [96].

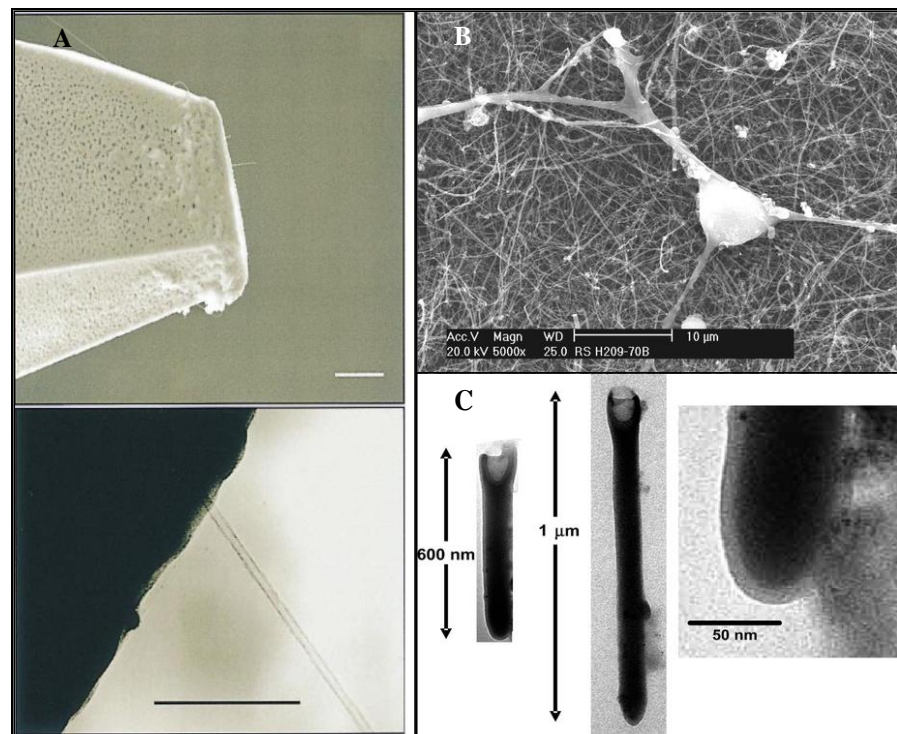


Figure 2.3. Applications of Carbon Nanotubes as A. AFM Probe tips [91], B. Substrates for neuronal growth [85] and C. Carbon Nanotube test tubes [89]

2.2. ASSEMBLY: TOP-DOWN AND BOTTOM-UP APPROACHES

This section discusses the assembly methods used for both top down and bottom up approaches, giving examples of CNT assembly with mentioned approaches and their application areas.

2.2.1. Top Down Approaches

Top Down approaches describe starting with a bulk material and trimming, cutting, shaping it to a desirable shape using lithography techniques, which include methods like X-ray lithography [97], photolithography [98], e-beam lithography [99] and ion beam lithography [100]. Basically lithography is creating a resist layer through the use of photons, e-beam etc. onto substrate material to create defined geometric shapes. There are two kinds of resists that can be used to generate a pattern, negative resist and positive resist [101]. Positive resist areas are removed upon exposure whereas negative resist areas removed if they are unexposed. This creates a pattern on the substrate surface. Depending on the source that removes the resist, lithography techniques divide into photolithography, e-beam lithography, etc. Generally, these methods are used to create 2D or 3D linear structures of CNTs into a defined pattern.

Photolithography uses photons with different light sources to create a pattern with magnification of light to create high-resolution patterns. It includes X-ray lithography and deep and near-ultraviolet photolithography. The resolution of the system depends on the wavelength of the light source, smaller wavelengths producing deep resolution on surfaces. However as the wavelength is reduced, the cost of manufacture increases.

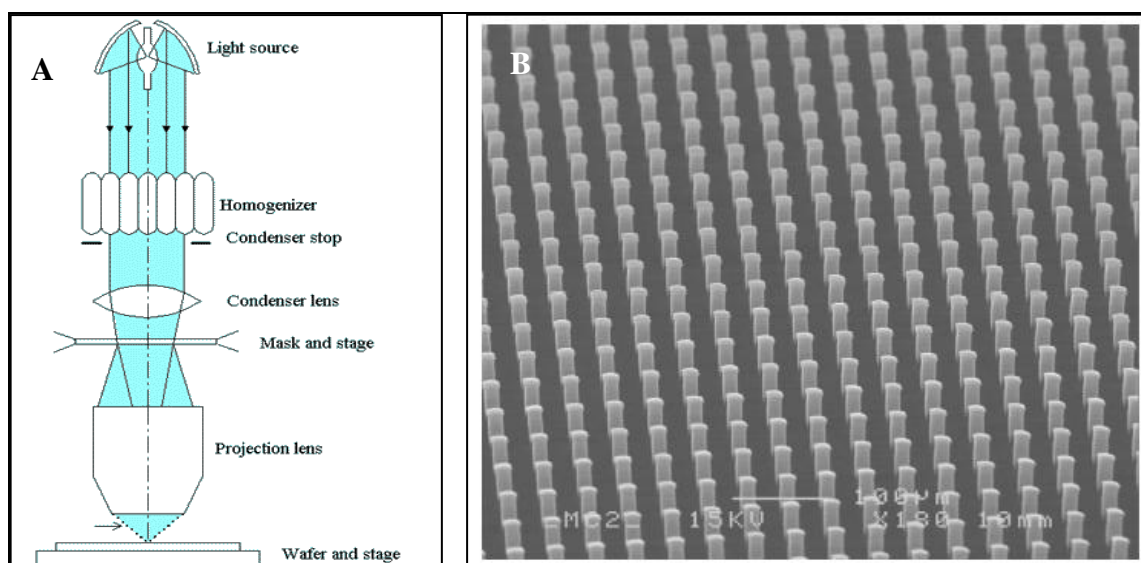


Figure 2.4. A. Schematic representation of photolithography [102] and B. CNT arrays using photolithography [103]

Figure 2.4 shows the schematic representation of photolithography and an example of CNT arrays produced using photolithography. In this particular example, photolithography is used to create Fe catalyst patterns and CNTs are grown on top of this catalyst, thus forming regularly shaped linear arrays that can be used in biosensing applications, microfluidic devices and transistors [103]. Another lithography technique is e-beam lithography. Since electron sources and electron optics are developed with Electron Microscopy, the equipment required for e-beam lithography is readily available with a resolution up to 1 nm. However, resolution limit is defined by scattered electrons. To prevent scattering problem, ion beam lithography is used, which incorporates ionized atoms focused with lenses. Their resolution decreases but they are more controlled. Lastly, X-ray lithography is an industry-based lithography where X-rays are used as light sources. However due to difficulties of obtaining high quality X-rays, this method is also limited.

These lithography techniques as well as others, require expensive equipment, trained operators and high operating cost. For this reason, it is desirable to create novel bottom up approaches with ease of production without a need for additional equipment and other expensive resources.

2.2.2. Bottom Up Approaches

Bottom up approaches are developed as an alternative to top-down approaches where the intermolecular forces, Van der Waals, hydrogen bonding and other non-covalent interactions gain importance [104]. It can be said that bottom up approaches are inspired from nature to create higher order structures. For these purposes, chemical interactions, liquid dynamics, evaporation patterns and biochemical affinity-bonding methods can be used. Bottom-up approaches can be divided into two main groups, assembly at liquid-liquid interface and assembly at solid-liquid interface. In this chapter, two of these methods as well as their subtopics are described with specific examples.

Self-assembly at Liquid-Liquid Interfaces takes advantage of two immiscible fluids forming an interface where nanoparticles stay and assemble based on their surface energies and chemistry [105]. In one example, CNTs are assembled into an ultra-thin film at water-hexane interface. Since CNTs lose their electronic and optical properties upon chemical treatment and functionalization, CNTs were dispersed in water with Sodium Dodecyl Sulfate(SDS) and hexane was placed on top of this solution. With this approach CNT-film is created without any chemical treatment and this structure can be used for flexible electronic devices [106].

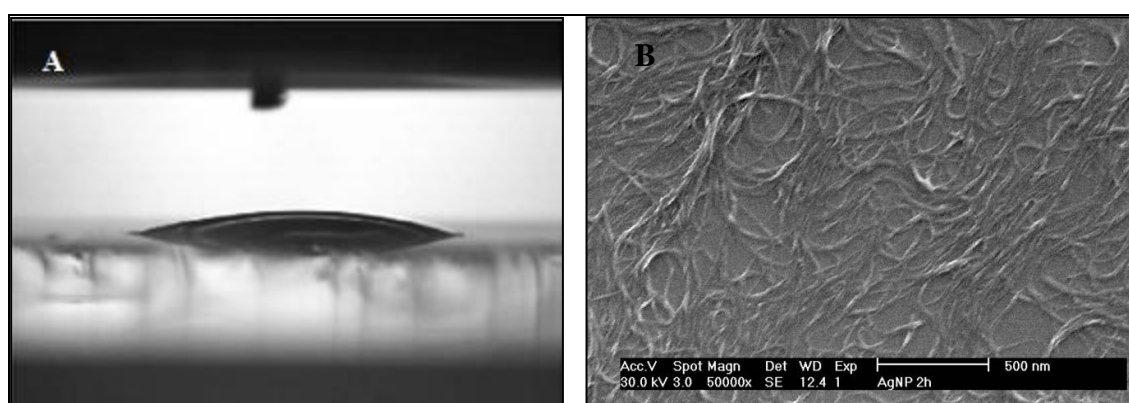


Figure 2.5. A. Ultrathin CNT film at water hexane interface and B. SEM image of CNT film assembled at water hexane interface [106]

Bottom up research is mainly focused on solid-liquid interfaces because unlike liquid-liquid interfaces, it promotes the intermolecular forces between chemical groups and offers a wide variety of interactions as well as promise of mediating and manipulating these interactions. These methods can create 1D, 2D and 3D structures by utilizing electrostatic interactions, hydrogen bonding, chemical bonds and hydrophobic interactions between NPs, liquid and solid. Self-assembly at solid-liquid interfaces can be divided into three methods: Self-assembly from a drying droplet, template assisted self-assembly and programmed self-assembly.

2.2.2.1. Self-assembly from a Drying Droplet

This approach involves the deposition of NPs on a solid surface from a suspension. When a droplet of a suspension is placed on a surface, the droplet tends to spread on the surface. However, the molecular or colloidal species bind quickly to the surface at solid-liquid-air contact line, which stops the spreading of droplet further. This is known as contact-line pinning, and results with a phenomenon called “coffee-ring” [107]. Since the solvent evaporation is faster at the contact line, the solvent molecules flow towards the contact line. This outward flow drags and jams all species in the droplet to the droplet edges. Dynamics in a drying droplet play important role for the distribution of species in the droplet area. Since this also influences the packing of colloidal nanoparticles in the droplet area, it has also has great influence on the performance of a surface-enhanced Raman (SERS) experiment employing colloidal noble metal NPs as substrates. The distribution of species [108]. As for CNTs, because of their tendency to stick together, their self-assembly behavior is different from other NPs. As droplet dries, CNTs do not travel to the edges of the droplet, because they stick to each other and they are heavy enough not being dragged to the edges, so as a result, the CNT concentration is highest at the center of the droplet and lowest at the edges [109]. This property of CNTs can be used to assemble individual CNTs onto surfaces, creating nanometer scale structures as opposed to large bundles. However, this phenomenon is not properly understood, so additional studies are needed in that direction.

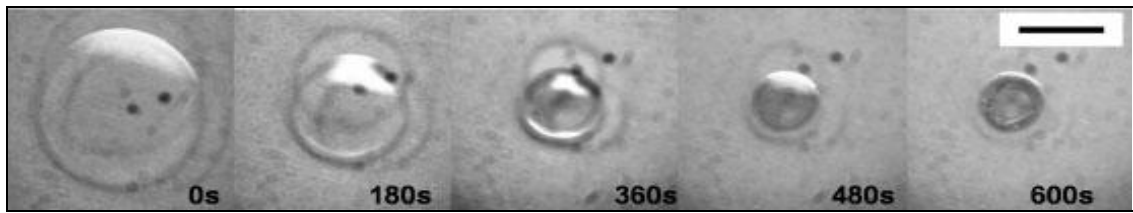


Figure 2.6. Image of drying pattern of CNT-F68 suspension where CNTs are concentrated at the center of the droplet [109]

2.2.2.2. *Template Assisted Self-assembly*

This approach involves creating a template before the assembly of the NPs so that NPs will be assembled into structures based on that template. This template can be created with lithographic approaches as well as different chemicals, solvents and polymers. One example is template assisted self-assembly of MWCNTs based on the concentric rings formed by polymer MEH-PPV with amazing regularity upon drying. This method creates a pattern on a large surface formed of ring structures and when MWCNTs are deposited onto these surfaces, they follow the pattern and deposit between the concentric rings created by MEH-PPV [110].

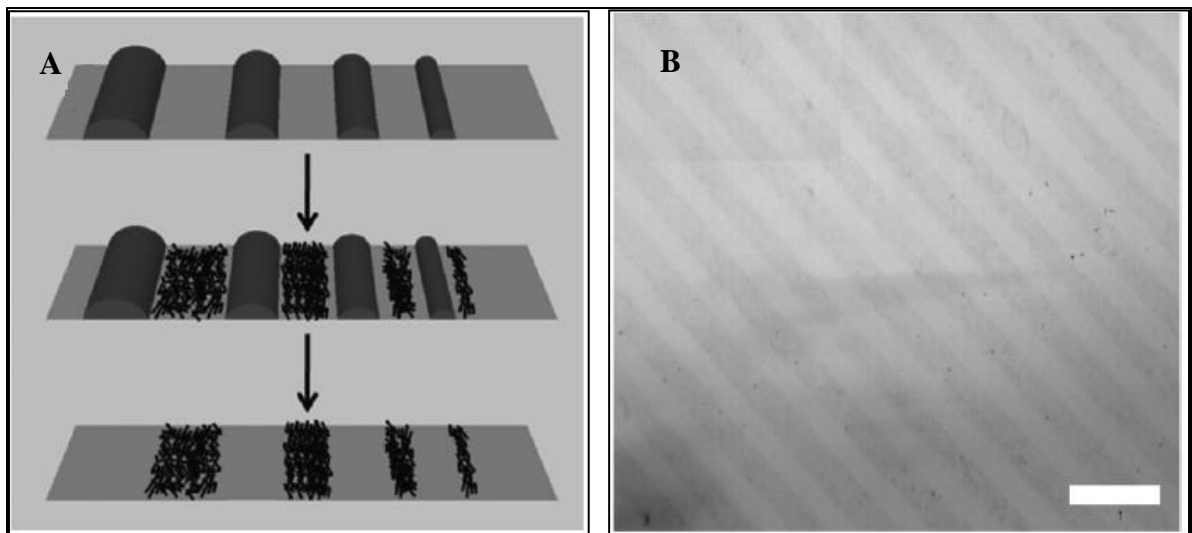


Figure 2.7. A. Representation of MEH-PPV concentric rings and CNT deposition on the surface and B. Optical image of the formed surface after MEH-PPV is removed [110]

2.2.2.3. Programmed Self-assembly

Among the various self-assembly techniques, programmed self-assembly stands out as a newly emerging concept but it has wide variety of applications and unlimited possibilities leading to formation of a plethora of nanoconstructs. Since this method uses the interactions of biomacromolecules DNA [111], RNA [112], peptides [113], carbohydrates [114], lipids [115] to assemble nanostructures, they can be applied and constructed in many laboratories without special equipment and with high throughput. Essentially, programmed self-assembly occurs continuously in nature with protein folding, DNA hybridization, membrane formation etc. What researchers do is, they utilize these interactions to bring NPs into a defined shape and pattern. Among various methods, DNA mediated self-assembly stands out as the most promising technique to assemble NPs.

DNA mediated self-assembly depends on Watson-Crick base pairing to assemble NPs. In general NPs are covalently bound to ODNs[116]. As complementary ODNs bind to each other, they bring NPs into defined nanostructures. DNA mediated self-assembly has many advantages. Their interaction pattern is well defined as opposed to peptides, they are relatively unaffected by the environmental pH. Individual ODNs are resistant to heat and pressure, however the nanostructures may dissociate upon the denaturation of double stranded DNA because of heat. ODNs are also easy to synthesize and control with a defined length and sequence. For these reasons, DNA mediated self-assembly flourished and has been the focus of intense research. At first, attempts were made to assemble conventional NPs like AuNPs where different sizes of NPs are bound to each other via DNA hybridization [117]. After that point, there were many studies for the assembly of AuNPs via DNA hybridization. QDs and MNPs were also subjected to intense research with DNA mediated self-assembly [118]. As NPs are assembled into defined structures, another topic, self-assembly of DNA itself has emerged with creation of DNA tiles [119] and other DNA based nanostructures [120]. NPs are incorporated into those structures, for example creation of periodic square like AuNP surfaces using DNA tiles for optical and plasmonic applications [121]. With the groundbreaking research done by Rothemund [122], DNA self-assembly reached its highest level. Rothemund used a M13 bacteriophage single stranded DNA and folded it with the help of small ODNs called stable strands to create a smiley face. He also showed how it is possible to create a structure with any shape using this method where he created rectangles, star shapes and triangles. Later, other researchers

working on DNA origami created spheres [123], scaffolds for nanoarrays [124], DNA tubules [125], letters [126] and a DNA box [127] that can only be opened upon a specific signal in the environment. Also, with the fluorescence molecules on its surface, the box emits different colors when it is closed and open. This technology provides both the controlled release and delivery of the drug and detection of diseases. CNTs are also incorporated into DNA mediated self-assembly and DNA origami approaches. One example is creating nanoribbons with DNA origami where CNTs can be placed to create a stable field effect transistor where DNA origami structure serves as a nanobreadboard [128].

In previous projects on ODN mediated self-assembly of AuNPs, it was observed that changing ODN linker concentration causes the assembly pattern of AuNPs change, so the same affect was investigated in this study, where DNA hybridization mediated assembly of SWCNTs was investigated upon changing ODN linker concentration that binds these SWCNTs together. It was hypothesized that as ODN linker concentration changes, SWCNTs will make different assembly patterns with each other. It was observed that at a specific ODN linker concentration, SWCNTs form carbon nanorings. Previously in literature, carbon nanorings were produced with chemical treatments and functionalization, which require special reaction conditions and time [129]. In this study it is shown that two different ODN bound SWCNTs can be brought together and form a nanoring structure by changing the concentration of the ODN linker molecule.

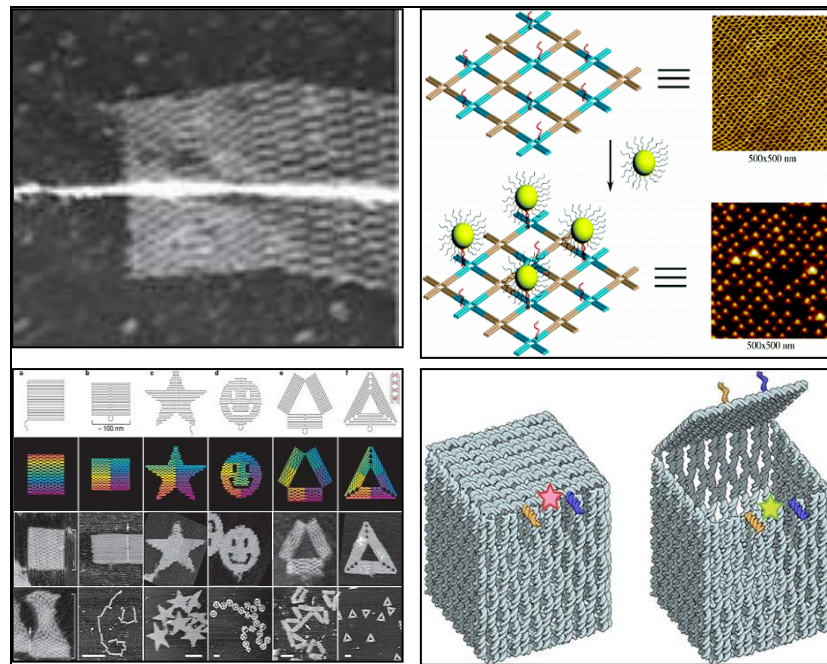


Figure 2.8. Nanostructures created based on DNA mediated self-assembly [121, 122, 127, 128]

3. MATERIALS

3.1. REAGENTS

SWCNTs were purchased from Sigma Aldrich (Taufkirchen, Germany), which contained tubes that are 0.7-0.9 nm in diameter. HNO₃, Magnesium Acetate, EDTA, Acetic Acid and Trizma base were also purchased from Sigma Aldrich (Taufkirchen, Germany). 1-ethyl-3-(3-dimethylaminopropyl) carbodiimide (EDC) is purchased from Fluka (Taufkirchen, Germany). Oligodeoxynucleotides (ODNs) were purchased from AlphaDNA (Quebec, Canada) as shown in Table 3.1.

3.2. OLIGODEOXYNUCLEOTIDES (ODNs)

ODNs were purchased in desalted form with a concentration of 200 nm and diluted to a final concentration of 100 μM with dH₂O. Table 3.1 shows the sequences of the ODNs used for the construction of carbon nanorings. D1, D2 are 5'-NH₂ terminated ODNs and D3, D4 are 3'-NH₂ terminated ODNs. After the chemical attachment of these ODNs to SWCNTs, D5, D6, D7, and D8 are used to bring the SWCNTs into patterns using them as linkers. These sequences are designed to see how different sequences of ODNs contributes to the nanoring formation as well as the effect of the length of ODN linkers. The sequences are given as from 5' end to 3' end.

Table 3.1. ODNs used for the formation of Carbon Nanorings

Label	Sequence (from 5' to 3')	Base number	Brand
D1	NH ₂ -(CH ₂) ₆ - AAAAAAAAAAATGTGTGGAGTTGGCTGTTAC GACTA	36	Alpha DNA
D2	CTCAGCCCAGGTTTCAGTTCTGGTCATAAAAAA AAAA-(CH ₂) ₆ -NH ₂	36	Alpha DNA
D3	NH ₂ -(CH ₂) ₆ -TTTTTTTTTTTTTTTTTTTT	20	Alpha DNA
D4	TTTTTTTTTTTTTTTTTTTT-(CH ₂) ₆ -NH ₂	20	Alpha DNA
D5	ATGACCAGAACTGAACCTGGGCTGAGTAGTC GTAACAGCCAACTCCACACAT	52	Alpha DNA
D6	ATGACCAGAACTGAACCTGGGCTGAGAAAAT AGTCGTAACAGCCAACTCCACACAT	56	Alpha DNA
D7	ATGACCAGAACTGAACCTGGGCTGAGAAAAA AAAATAGTCGTAACAGCCAACTCCACACAT	61	Alpha DNA
D8	AAAAAAAAAAAAAAAAAAAAAAAAAAAAAAAAA AAAAAAAAA	40	Alpha DNA

According to this experimental setup ODNs D1 and D2 are connecting in the presence of ODN linkers D5, 6 and 7. Among these ODN linkers D7 has 9 Adenosine molecules used as a spacer, D6 has 4 Adenosine molecules and D5 has none to see the effect of ODN linker length on assembled nanostructures. ODNs D3 and D4 consist of only single bases and do not contain 10 Adenosine molecules to distance DNA hybridization from SWCNTs. They are connected by ODN linker D8 which consists of 40 Adenosine molecules.

4. METHODS

4.1. CARBOXYLIC ACID FUNCTIONALIZATION OF CARBON NANOTUBES

Carbon nanotubes are functionalized using the acid reflux method. A 5 mg of SWCNTs was dissolved in 5 ml dH₂O and sonicated for 30 minutes. Then, they were treated with 2.3 ml of 4 M HNO₃ for four hours in reflux. The acidic solution was transferred into a crucible and evaporated with an incubator. A small volume of dH₂O was added to the crucible and SWCNTs were taken into eppendorf tubes for further activation. Figure 4.1 shows the comparison Raman spectra of pristine SWCNTs and carboxyl functionalized SWCNTs. On a SWCNT spectrum there are four distinct bands that are associated with properties of SWCNTs. These are the D band located at 1340 cm⁻¹, the G band located at 1590 cm⁻¹, G' band located between 2500-2700 cm⁻¹, and the RBM bands between 350-150 cm⁻¹. However, the band at 320 cm⁻¹ that is present in all samples, is attributed to the CaF₂ slides the samples were deposited on. The carboxylation of SWCNTs was assessed based on the ratio of D and G bands peak heights, since D band represents the defects of SWCNTs graphite-like structure, it is a direct indicator of functionalization. D/G ratio was calculated as 0.18 for pristine SWCNT and 0.43 for carboxyl functionalized SWCNTs shown in Figure 4.1. There is also a shift in the bands that indicates a change in the electrical properties of SWCNTs due to surface functionalization and disruption of electronic properties.

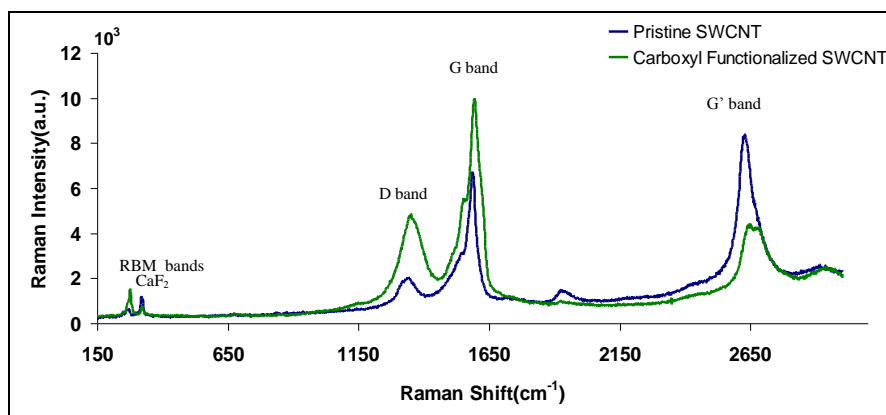


Figure 4.1. Raman spectra of pristine SWCNT and carboxylated SWCNT.

Figure 4.2 shows the comparison of FTIR spectra of pristine and carboxylated carbon nanotubes. There are multiple bands that indicate the carboxylation of SWCNTs. The broad peak at 3200 cm^{-1} corresponds to $-\text{OH}$ vibrations coming from carboxyl groups. The region between 1800 and 1500 cm^{-1} show high frequency vibrations due to carboxylation. Broad peak centered at 1733 cm^{-1} attribute to $\text{C}=\text{O}$ stretching vibrations of carboxyl and carbonyl groups. Another broad peak with high frequency vibrations centered at 1557 cm^{-1} indicates the conjugation between $\text{C}=\text{O}$ groups and $\text{C}=\text{C}$ groups. The shoulder at 1317 cm^{-1} indicates the presence of $\text{C}-\text{OH}$ groups. The peak at 1260 cm^{-1} corresponds to $\text{C}-\text{O}$ stretching vibrations as well as $1212\text{-}1175\text{ cm}^{-1}$ peak with a shoulder at $1112\text{-}1038\text{ cm}^{-1}$.

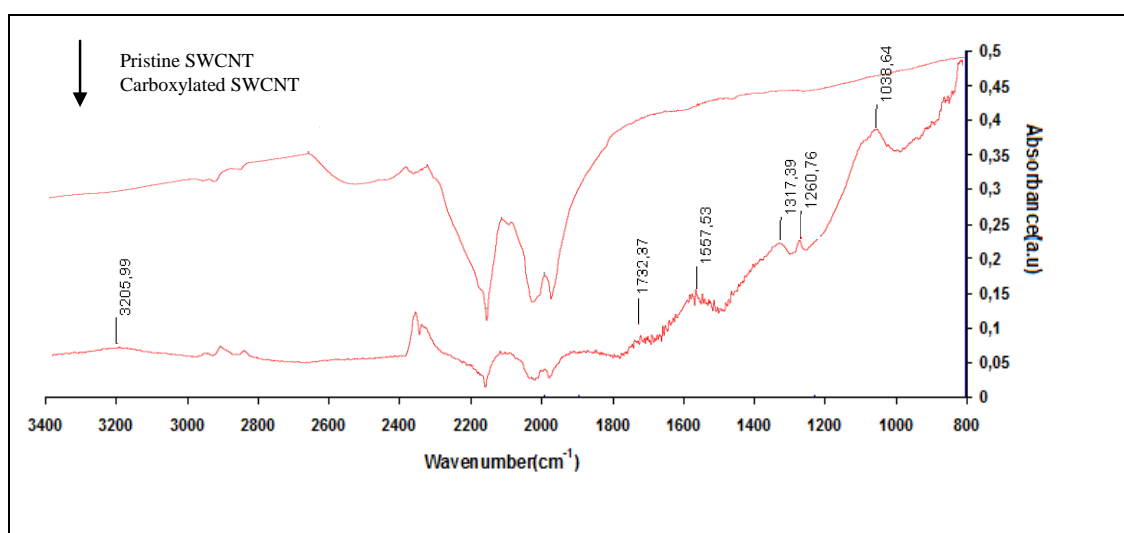


Figure 4.2. FTIR spectra of pristine SWCNTs and carboxyl functionalized SWCNTs.

4.2. CHEMICAL ATTACHMENT OF AMINE TERMINATED OLIGONUCLEOTIDES TO SINGLE WALLED CARBON NANOTUBES

The carboxylated SWCNTs are covalently bound to amine terminated ODNs via an carboamide bond. A $100\text{ }\mu\text{L}$ of carboxylated SWCNT is mixed with $5\text{ }\mu\text{L}$ of $100\text{ }\mu\text{M}$ ODNs D1, D2, D3 and D4 in the presence of 1 mg EDC, which is a crosslinking agent between carboxyl and amine groups. The SWCNTs are incubated overnight in the presence of EDC and then centrifuged to remove excess EDC and ODNs. The reactions involved in this process are illustrated in Figure 4.3. The pellet, containing ODN bound SWCNTs are

suspended with TAE Mg^{+2} buffer (40 mM Tris base, pH 8.0, 20 mM acetic acid, 2 mM EDTA and 5 mM Magnesium Acetate) and stored at $+4\text{ C}^{\circ}$ for further use.

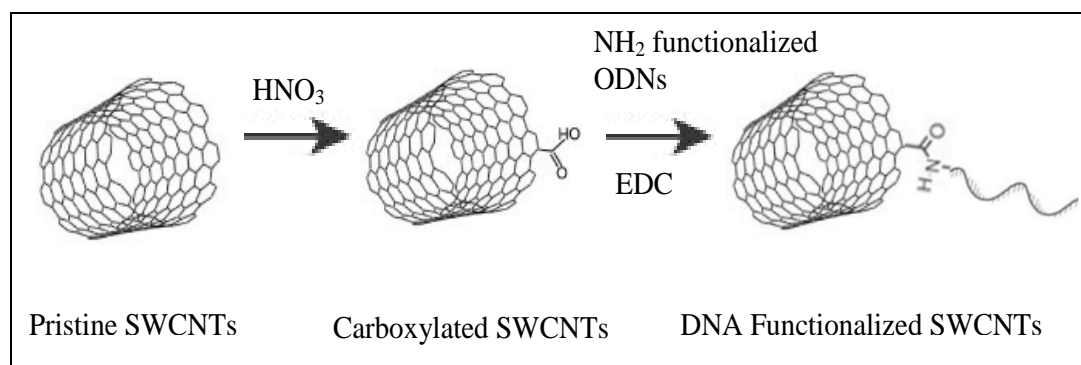


Figure 4.3. DNA functionalization of SWCNTs in the presence of EDC

4.3. CONSTRUCTION OF NANOSTRUCTURES

After the covalent binding of ODNs to SWCNTs via an amide bond, the functionalized SWCNTs are linked to each other by using complementary linker ODNs. It was hypothesized that in dilute samples with excess linker ODN concentration, SWCNTs tend to assemble onto themselves, creating small circular shapes by joining two ends together. Two different ODNs bound SWCNTs are linked to each other with the help of a ODN linker.

In order to investigate parameters affecting the formation of carbon nanorings, the experiment is designed as two parts. In the first part, nanoring structures are constructed with SWCNT-D1 and SWCNT-D2 using linkers D5, D6 and D7. The linker ODNs possess sticky ends for D1 and D2. These ODN linkers have different lengths to observe the influence of linker length to the formation of nanorings. To investigate the effect of linker ODN concentration, D5 was added to the solutions in varying concentrations. To construct these nanorings a $10\ \mu\text{L}$ of D1 and D2 bound SWCNTs are mixed in three separate test tubes. Then, $5\ \mu\text{L}$, $10\ \mu\text{L}$ and $20\ \mu\text{L}$ linker ODN solutions are added to the test tubes, to change the linker concentration, respectively. Then magnesium acetate buffer was added to the suspension to make final volume $200\ \mu\text{L}$. The same procedure is repeated for other sets with linkers D6 and D7, respectively. ODNs D3 and D4 were used to investigate the effect

of sequence specificity in nanoring formation. These ODNs were composed of Poly-T sequences and were brought together in the presence of Poly-A ODN linker D8. For this reason, they can hybridize with ODN linker from different points. These ODN bound SWCNTs were assembled as described above and the structures are analyzed under AFM.

4.3.1. Raman Instrumentation

Raman Spectroscopy experiments are undertaken with a Renishaw inVia reflex Raman microscopy system was used. The system was automatically calibrated against a silicon wafer peak at 520 cm^{-1} . An argon ion laser at 514 nm was used with a $\times 50$ objective (numerical aperture is 0.75) with laser power of 200 mW.

4.3.2. FTIR Analysis

FTIR analysis was done by Thermo Scientific Smart iTR in ATR mode with a diamond plate and ZnSe lens. Dehydrated Carbon Nanotubes are used to characterize functionalization and DNA binding.

4.3.3. Scanning Electron Microscopy Analysis

SEM measurements were performed with a Karl Zeiss EVO 40 model SEM instrument operating at 20 kV.

4.3.4. Atomic Force Microscopy Analysis

The AFM analyses were performed with a Park SYSTEMS XE 100 Atomic Force Microscopy (Park Systems Corp. KANC 4F, Iui-Dong, 906-10 Suwon 443-766, Korea). The images are taken at room temperature with non-contact mode using conventional silicon nitride tips. The resonance frequencies varied between 200 and 300 kHz and the scanning rate of the images was 0.5 Hz for lower magnifications and 1 Hz for higher magnifications.

5. RESULTS AND DISCUSSION

5.1. CHARACTERIZATION OF OLIGONUCLEOTIDE BINDING TO SINGLE WALLED CARBON NANOTUBES

The ODN bound SWCNTs were characterized using FTIR and Raman Spectroscopy. Figure 5.1 shows the change in D and G bands. After carboxylation, D/G band ratio was 0.43, which indicates the loss of sp² hybridization of carbon atoms and presence of carboxyl groups. When the ODN binds to SWCNTs covalently, D/G ratio drops to 0.35 and SWCNTs form aggregates, indicating the change in surface chemistry on SWCNTs upon DNA crosslinking.

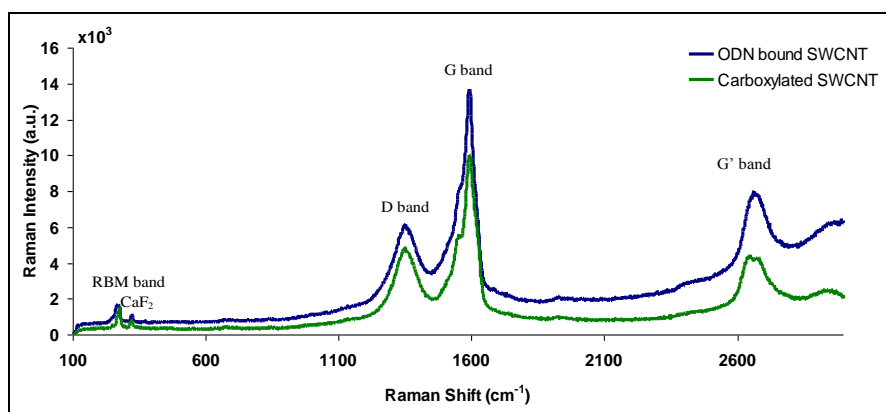


Figure 5.1. Raman spectra of ODN bound SWCNTs

Figure 5.2 shows FTIR spectra of ODN bound SWCNTs. A broad band at 3300 cm⁻¹ indicates presence of -OH stretching of water. The region between 3000-2800 cm⁻¹ indicates C-H stretching coming from the carbohydrate ring in DNA structure. The peak at 1640 cm⁻¹ indicates the presence of amide bond and the peaks in the range of 1700-1600 cm⁻¹, which shows the presence of other amide bonds and carboxyl groups, can not be clearly observed due to overlapping intense bands originating from ODNs. Peaks at 1560, 1530, 1485, 1467 and 1378 cm⁻¹ relate to different vibrations and stretching of DNA bases. The peaks between 1200 and 1150 cm⁻¹ show the presence of phosphodiester bonds in the

DNA backbone. The peaks at 1089 and 971 cm^{-1} relates to PO_2^- stretch and PO_4^{2-} vibrations of nucleic acids respectively. The peak at 1057 cm^{-1} is C-O stretch of DNA structure. Overall these results demonstrate that ODNs are attached to the SWCNTs. Note that several centrifugation procedures is applied to remove the nonspecifically bound ODNs. The strongest evidence is that the peak at 1640 cm^{-1} shows that ODNs are covalently bound to SWCNTs via an amide bond [130].

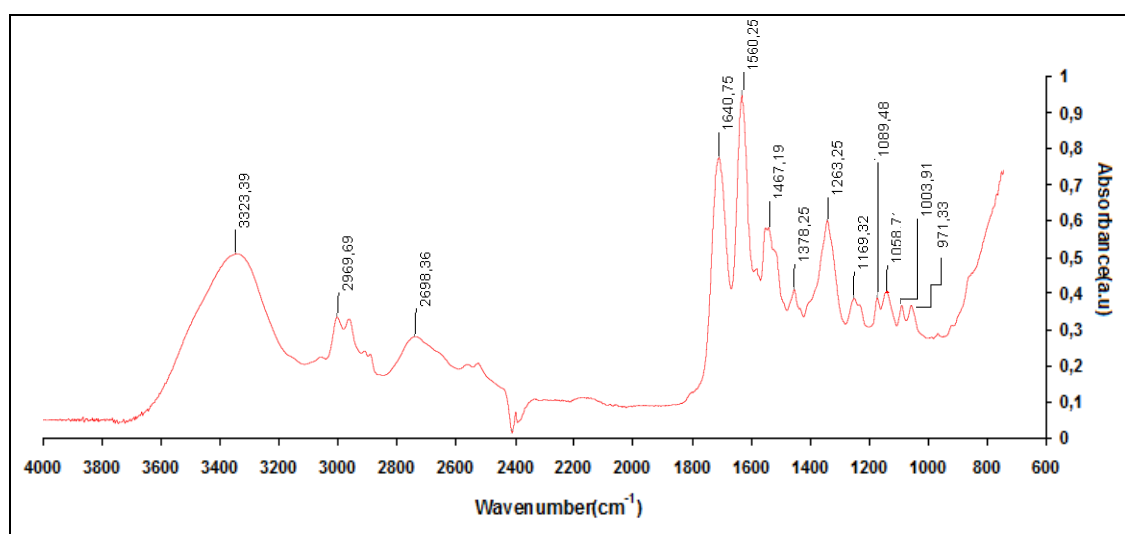


Figure 5.2. FTIR spectra of DNA bound Carbon Nanotubes

5.2. CONSTRUCTING NANORINGS USING ODN LINKERS

This section outlines the construction of nanorings from ODN-bound carbon nanotubes. Nanoring structures were assembled in the presence of an ODN linker and observed under AFM. To determine the factors affecting nanoring formation, different concentration of ODN linkers were used to assemble ODN-bound CNTs. In addition, the effect of ODN linker length was investigated by using different lengths of ODN linkers. Lastly, ODN sequences that were bound to the CNTs were changed to see if the specificity of this sequence contributes to the formation of nanorings.

5.2.1. Constructing Nanorings with ODNs D1 and D2

Nanorings were constructed with D1 and D2 at different ODN linker concentrations and lengths using ODN linker D7 as illustrated in Figure 5.3. ODNs D1 and D2 contain 10 Adenosine molecules between the SWCNT and the sequences that hybridize with D7. These adenosine molecules are not hybridized and they distance the hybridized sequences from SWCNTs. They also give the structure flexibility. ODN linker D7 also contains 9 Adenosine molecules in the middle, which was used to create a distance between ODN-SWCNT complexes and to give the structure flexibility.

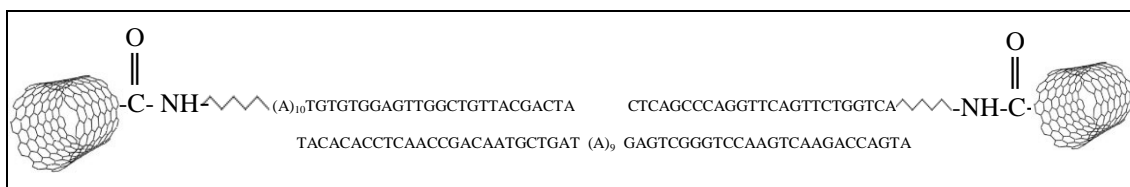


Figure 5.3. Representation of hybridization of ODNs D1 and D2 with ODN linker D7.

It was observed that the prepared solutions formed aggregates on surfaces since ODN-SWCNT concentration was very high. For this purpose, in accordance with the literature, SWCNTs were diluted with a factor of $1:10^8$ in 4 steps in order to prevent their aggregation (debundling) [131]. To explain the dynamics leading to formation of nanoring structure, it is proposed that sticky ends of ODNs attached to SWCNTs are brought together through the hybridization of the ODN linker from two ends as illustrated in Figure 5.4. This creates a single SWCNT ring that acts as a seed. After the formation of the seed, because of the affinity of SWCNTs towards each other, they form bundles by sitting on top of each other during the drying process. As different concentration of ODN linker molecules are tried, it was seen that the nanoring structures only form in the presence of 5 mM of ODN linker molecule.

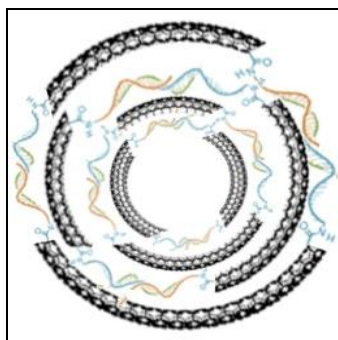


Figure 5.4. Proposed DNA mediated nanoring model(not in scale)

Although the ODN-SWCNTs are dispersed in water fairly good, it is still possible for them to form aggregates. When SWCNTs are oxidized in an acid, the possible oxidation locations are ends or defects on the wall. Considering that the most of the attachment is achieved at the ends of the SWCNTs, they will still have the tendency to form aggregates. This tendency becomes more dominant in the presence of increased number of SWCNTs. When there is a big crowd of them, they may fold onto each other creating amorphous aggregates. Therefore, dilution can help to form ring structures by attracting SWCNTs around themselves. This creates nanoring structures that can be seen from Figure 5.5. The structure constructed with the hybridization of from D1-SWCNTs and D2-SWCNTs with the linker D7. It shows the nanoring structures that are around 1 nm high, which is about to height of both SWCNTs and ODN.

Figure 5.5 also shows that some ring structures are incomplete whereas other structures have aggregates on certain parts. There are also round aggregates that don't have any holes in the middle, indicating these structures did not assemble properly to create nanorings.

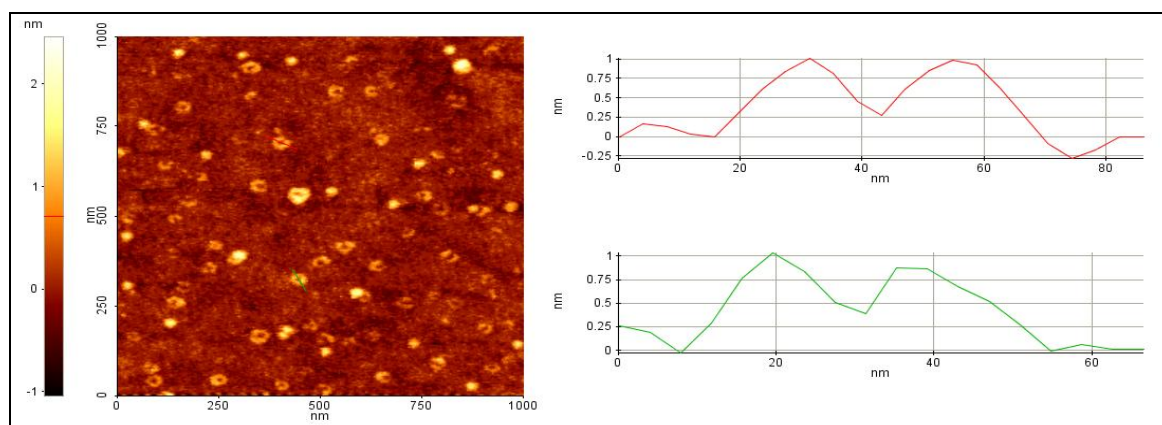


Figure 5.5. Carbon nanoring structures formed with ODNs D1 and D2 and ODN linker D7 on glass surfaces.

A glass surface is covered with free silanol (Si-O-H) groups. However, silanol groups do not cover the surface uniformly. This non-uniform distribution may influence the formation of nanorings on the surface since ODNs can make hydrogen bonds with the free silanol groups. As seen, the rings are not perfect on the glass surface. Therefore, the experiments were repeated on a much smoother and hydrophilic mica surface. Since glass surface is not smooth. Figure 5.6 shows the formation of carbon nanoring circles on mica surfaces. Compared to the nanoring formation on glass surfaces, mica surface shows nearly perfect structures with no incomplete circles, no aggregation and no unbound SWCNTs. Both surfaces are hydrophilic but the surface roughness could also be important. The glass surface is much rougher than mica. The hydrophilic nature of mica forces SWCNTs to find each other instead of sticking to a hydrophilic and rough surface as it is in the case of glass surface so they are likely to form nanoring structures with an ordered way.

While nanorings were formed on glass and mica surfaces since they were hydrophilic, we were unable to observe nanorings on TEM grids because carbon film supported grids were hydrophobic and nanorings did not assemble on these grids. Figure 5.6 shows that on mica surfaces the height of SWCNTs are increased to 5 nm accompanied with an increase in their size, which is around 200 nm as opposed to 50 nm. This is because the SWCNTs tend to stick to each other more on a highly hydrophilic mica surface and form larger nanoring structures as opposed to those on the glass surfaces.

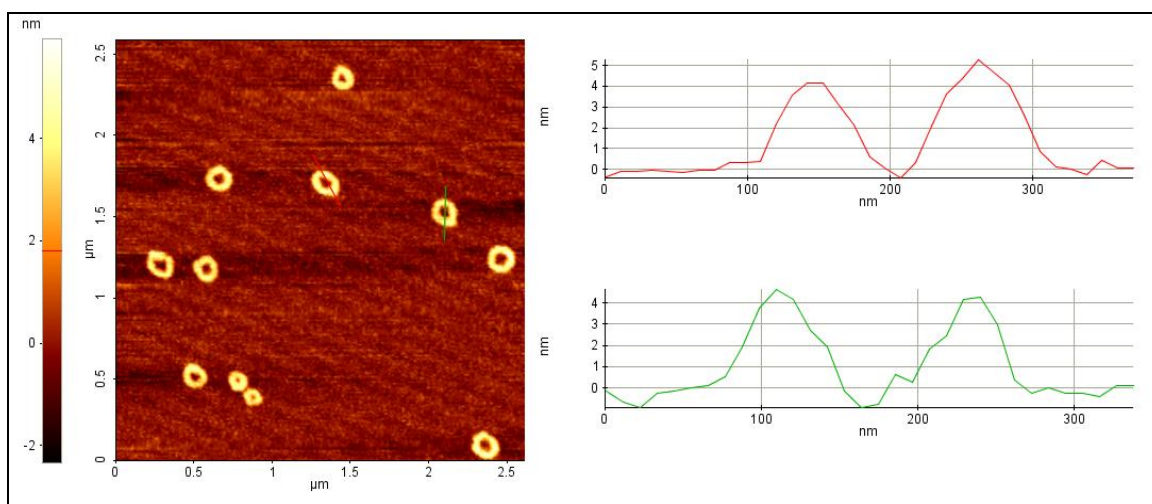


Figure 5.6. Carbon nanoring structures formed with ODNs D1 and D2 on mica

As presented in Figure 5.7, when a droplet of suspension containing SWCNT is placed on a surface, evaporation starts from the sides and the water molecules move outwards as explained earlier. However, since the affinity of SWCNTs for each other is much higher than their solubility in water, SWCNTs remain together and shrink into a small area at the center of the droplet forming a highly concentrated region. It is not possible to acquire images of individual SWCNTs or nanorings from this highly concentrated region. However as the droplet dries, individual SWCNTs are adsorbed to the surface starting from the contact line of the droplet to the highly concentrated region of the dried droplet at the center. Interestingly, this drying process creates a gradient of concentration on the surface, lowest concentration of SWCNTs at contact line and it becomes increasingly higher as moved to the highly concentrated region in the middle. What is observed in such a case that the nanorings that are formed changes in size and height when the images were acquired from regions closer to center. Nanorings at the contact line has about 1-2 nm height in a typical droplet, as moved closer to the center, they become higher and the hole of the nanorings become smaller. This is due to deposition of many SWCNTs on top of each other that is added to nanoring seed from all sides. Figure 5.8 shows 4-6 nm high nanorings with a general view and Figure 5.9 is a close up of the nanoring structure.

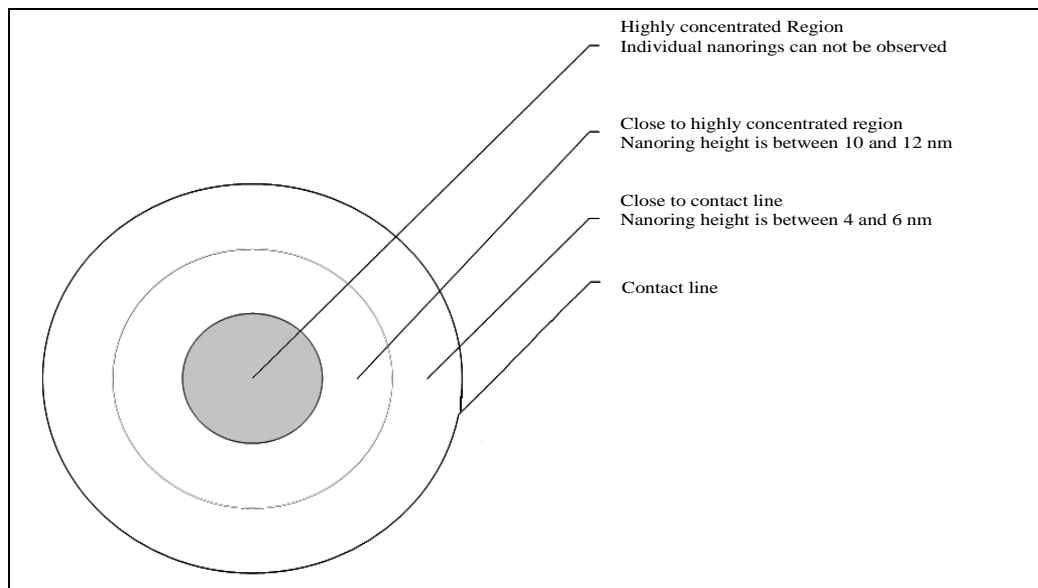


Figure 5.7. Schematic presentation of drying pattern of SWCNT samples

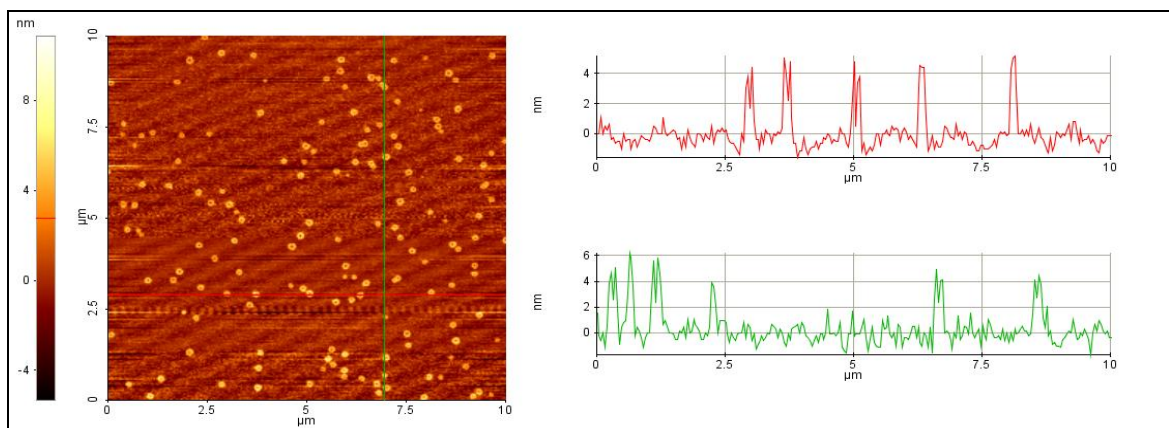


Figure 5.8. AFM image of 4-6 nm high carbon nanorings between contact line and highly concentrated region

Figure 5.9 clearly shows detailed features of nanorings. As the figure and line analysis of the image shows, these nanorings are about 200 nm in diameter and 4-6 nm in height. Even though, there are some circles that are filled up and some smaller nanorings, these are due to the difference between the lengths of individual SWCNTs that compromise the nanoring structure. As the images are acquired closer to the concentrated region, nanoring height increases and the hole in the middle becomes barely visible and the height of nanoring

becomes around 10 nm. Figure 5.10 shows such nanoring structures where it is hard to see the hole in the middle, but based on the line analysis, there is a gap between two sides.

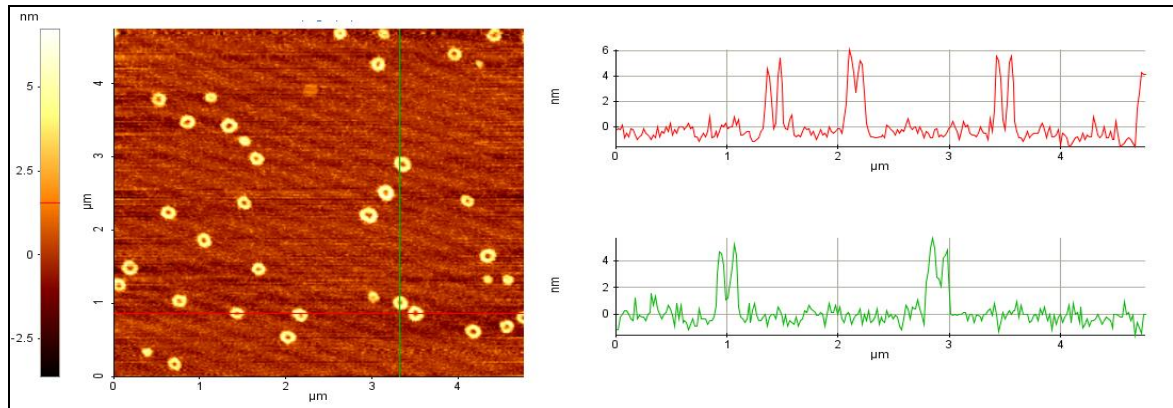


Figure 5.9. Close up AFM image of 4-6 nm high carbon nanorings between contact line and highly concentrated region

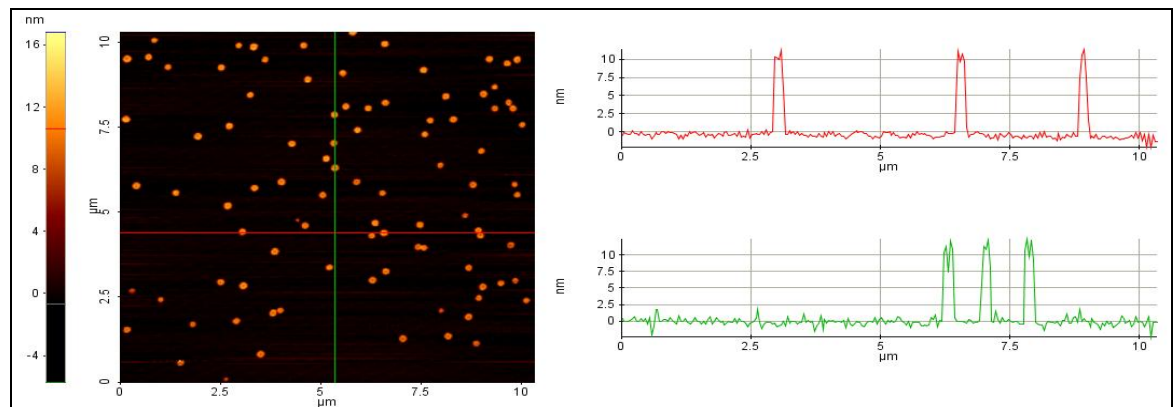


Figure 5.10. AFM image of 10-12 nm high carbon nanorings closer to highly concentrated region

To increase the visibility, the contrast of images are increased and presented in blue as seen in Figure 5.11. This image was acquired from a similar region where nanoring height is above 10 nm and the holes in the middle can be seen. Again, line analysis indicates the holes are there, but they are small in size as compared to the holes of 4-6 nm high nanorings.

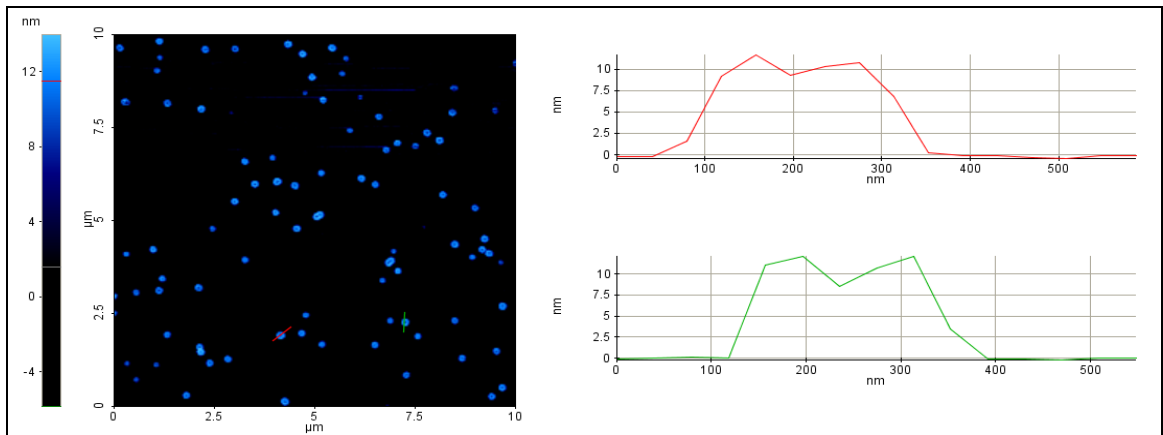


Figure 5.11. AFM image of 10-12 nm high carbon nanorings closer to highly concentrated region (shown in blue for better visualization)

Figure 5.12 shows close up of the 10-12 nm high carbon nanoring structures where the holes can be seen. Interestingly, some holes are filled more than the others, and those closer to concentrated region has smaller holes. Overall these results indicate that as nanorings begin to assemble, the immediate vicinity of the nanoring seed plays essential role on the shape and size nanorings will take. If there is too much ODN-SWCNTs, they may become higher and their holes tend to close up. If there isn't too much SWCNT, the size of the nanorings significantly decreases as their building blocks are not present.

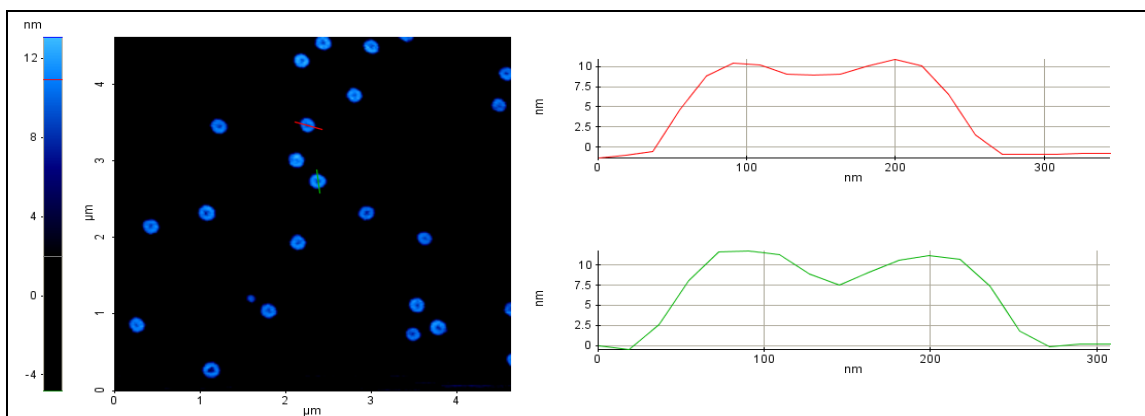


Figure 5.12. Close up AFM image of 10-12 nm high carbon nanorings closer to highly concentrated region (shown in blue for better visualization)

As discussed above, the concentration of SWCNTs could be an important parameter on the formation of nanorings, but also after the nanorings are formed, their proximity to each other creates other patterns, which are hard to observe since there is a fine line between the formation of nanorings and aggregation of SWCNTs into amorphous shapes. However, during the drying process, two nanorings can encounter and combine with each other as shown in Figure 5.13 indicated in red line analysis where there are three peaks caused by the walls of nanorings and two holes in the middle.

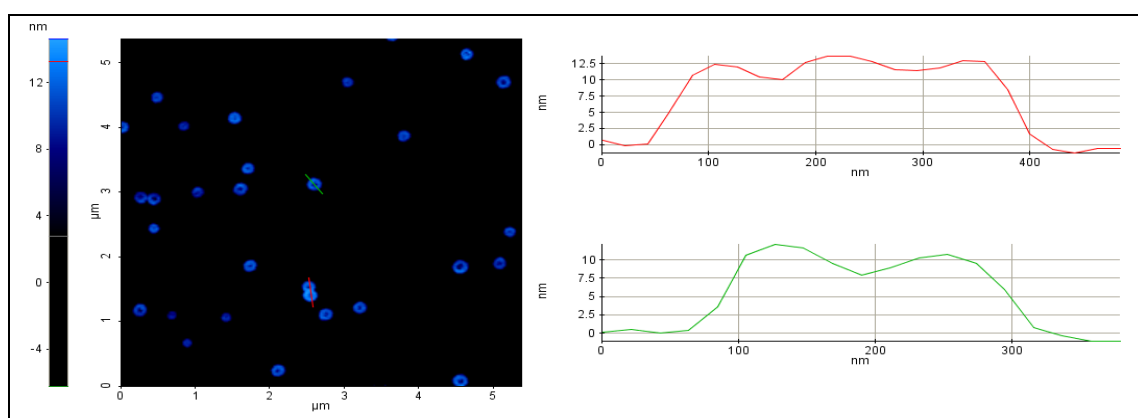


Figure 5.13. AFM image of combination of two nanorings indicated in red line analysis

In their pristine form, SWCNTs have various lengths, but their acid treatment for carboxylation reduces this size. For this reason, most of the ring structure that is observed are limited in size and are not composed of long SWCNTs. Another factor is the majority of long SWCNTs tend to pack into highly concentrated region since their assembly with DNA is much harder than that of short SWCNTs. Even though it is rare to encounter, there are nanorings that are composed of long SWCNTs as shown in Figure 5.14, which has an overall diameter of 1 μm and a height of 2 nm, which indicates, it is composed of a SWCNT layer rather than SWCNTs on top of each other. The thickness of nanorings walls varies, but they are around 100-150 nm.

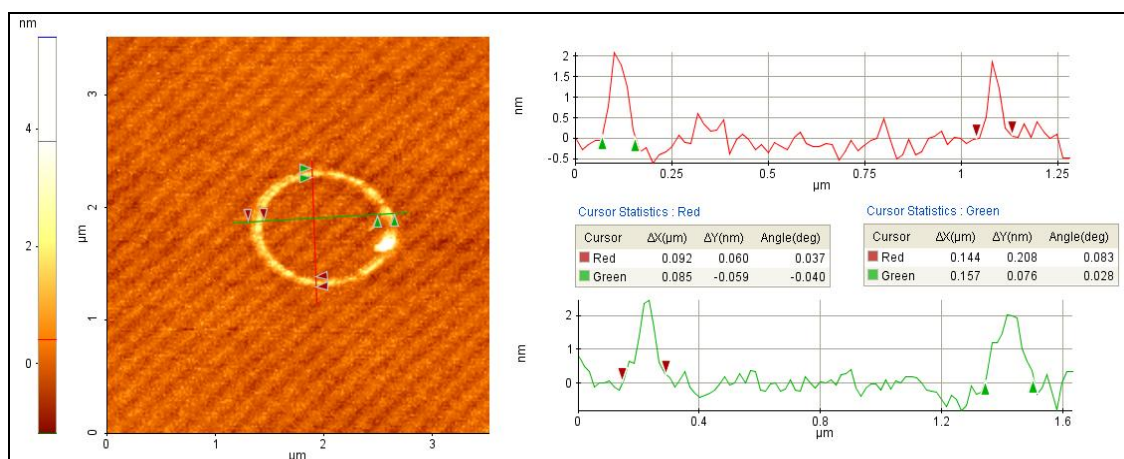


Figure 5.14. AFM image of nanoring structure composed of long SWCNTs

5.2.2. Effect of ODN Linker Concentration on Nanorings

As indicated above, the rings were formed only in the presence of 5 mM ODN linker concentration. To see how the ring structures were affected with 2,5 mM and 10 mM ODN linker concentrations, these samples were prepared. As can be seen from Figure 5.15, with 2,5 mM ODN linker, it is not enough for SWCNTs to form nanorings independently. Therefore, they tend to form incomplete nanoring structures, or several ring structures that form aggregates with a height of 1-1.5 nm, which indicates the SWCNTs are a single layer, they are not sitting on top of each other. However, at the upper side of the image, there are two larger SWCNT networks composed of formation of many incomplete nanorings with a height of 2 nm.

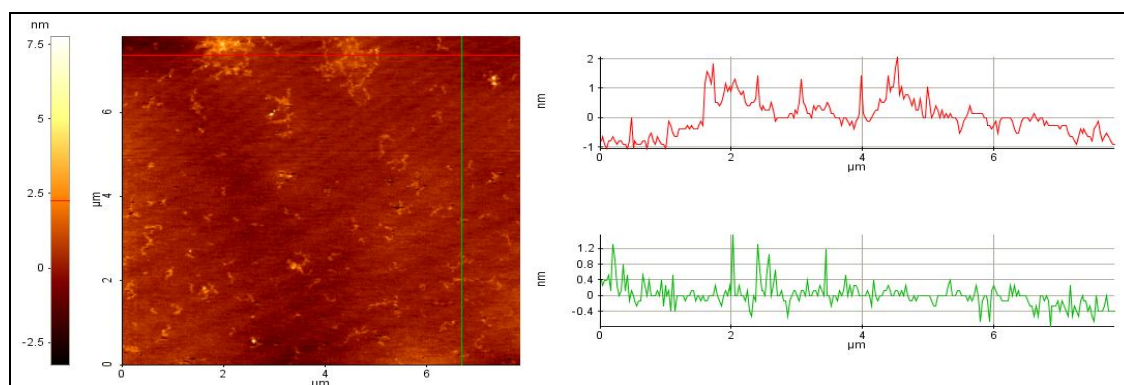


Figure 5.15. AFM image of incomplete nanorings and aggregates

Figure 5.16 shows a closer image of the above figure where half formations of nanorings and longer aggregates were seen because ODN concentration is not enough to bend SWCNT aggregates into full circles close the gaps.

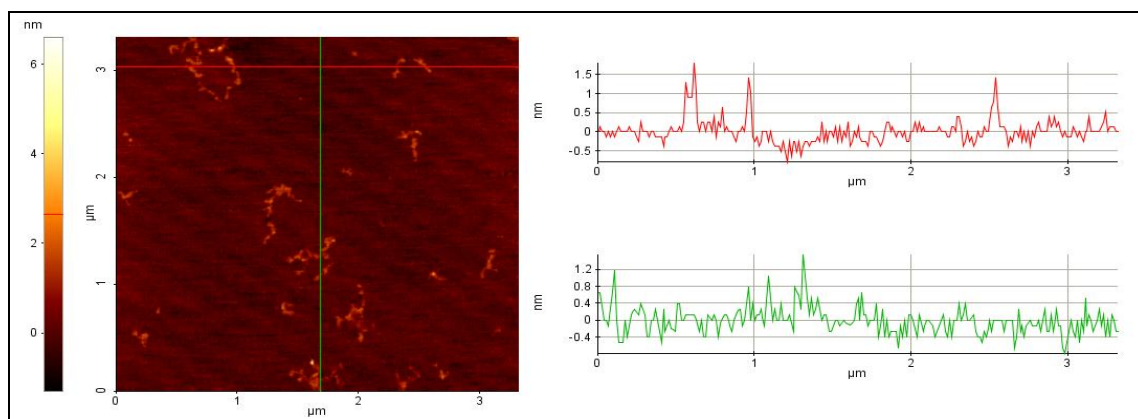


Figure 5.16. Closer AFM image of incomplete nanorings and aggregates

In order to investigate the influence of the increased ODNs, 10 mM of ODN linker, D7 is used to form nanoring structures. Figure 5.17 shows comparison of the AFM images obtained with addition of 2,5 and 10 mM ODN linker. As seen, lower concentration of ODN causes bending but forms incomplete nanorings. When 10 mM ODN linker is used, the nanoring structures are formed but the rings appear to be deformed and smaller than the nanorings constructed with the addition of 5 mM ODN linker. The addition of too much of ODN linker may also interact through non-specific interaction with SWCNTs, which may influence the ring formation in a negative way since for the proposed mechanism it is necessary for SWCNTs to maintain their hydrophobic properties through their body. When the SWCNTs get better dispersed in water with the excess of added ODN linker, their affinity to assemble onto the seed ring structure gets more difficult. As shown on the image, SWCNT circles are distorted and smaller, and in some cases, the circle is not formed. In conclusion, it can be said that excess ODN linker concentration decreases the efficiency of nanoring formation.

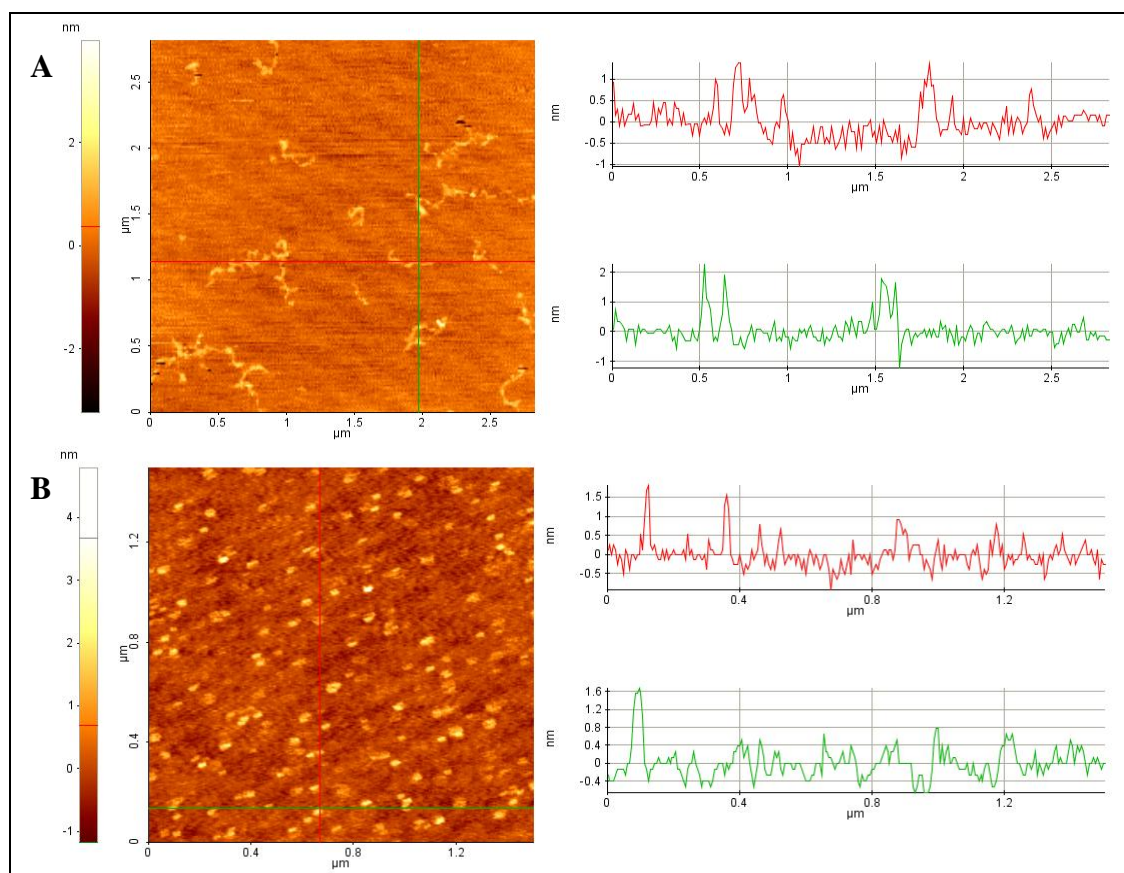


Figure 5.17. AFM image of A. Incomplete nanorings and aggregates formed by 2,5 mM ODN linker and B. Deformed nanorings due to incomplete aggregation formed by 10 mM ODN linker

Over all, these results indicate that there is an optimum concentration for the formation of carbon nanorings. The low concentration of ODN linker results with incomplete nanorings and featureless aggregates, the high concentrations of ODN linker results with deformed nanorings.

5.2.3. Effect of ODN Linker Length on Nanorings

In previous sections, the nanorings were constructed using ODN linker D7, which is the longest strand with a length of 61 bases corresponding to about 24 nm. The ODN linker length may play a role for the formation of nanorings, so 52 base pair long D5 and 56 base pair long D6 were used as ODN linker molecules were constructed and their effect was observed with AFM. D7 ODN linker had 9 Adenosine molecules that acts as a spacer and

distances ODN-SWCNTs. As shown in Figure 5.18, D6 has a spacer consisting of 4 Adenosine sequences and D5 has no spacer Adenosine that distances ODN-SWCNTs from each other. Since shorter ODN linkers fail to keep SWCNTs at a proper distance from each other they can not assemble into individual nanorings. Also, as the number of Adenosine bases used as a spacer decreases, the flexibility of the ODNs decreases and ODN-SWCNTs can not bend to form nanorings. This lack of distance and flexibility causes SWCNTs to assemble onto each other, creating these round shaped aggregates with between 10-20 nm height in both D5 and D6 ODN linkers as shown in Figure 5.19. These results indicate that ODN linker length and flexibility play an essential role during nanoring formation by distancing and bending ODN-SWCNTs.



Figure 5.18. Representation of hybridization of ODNs D1 and D2 with ODN linkers A) D5 and B) D6

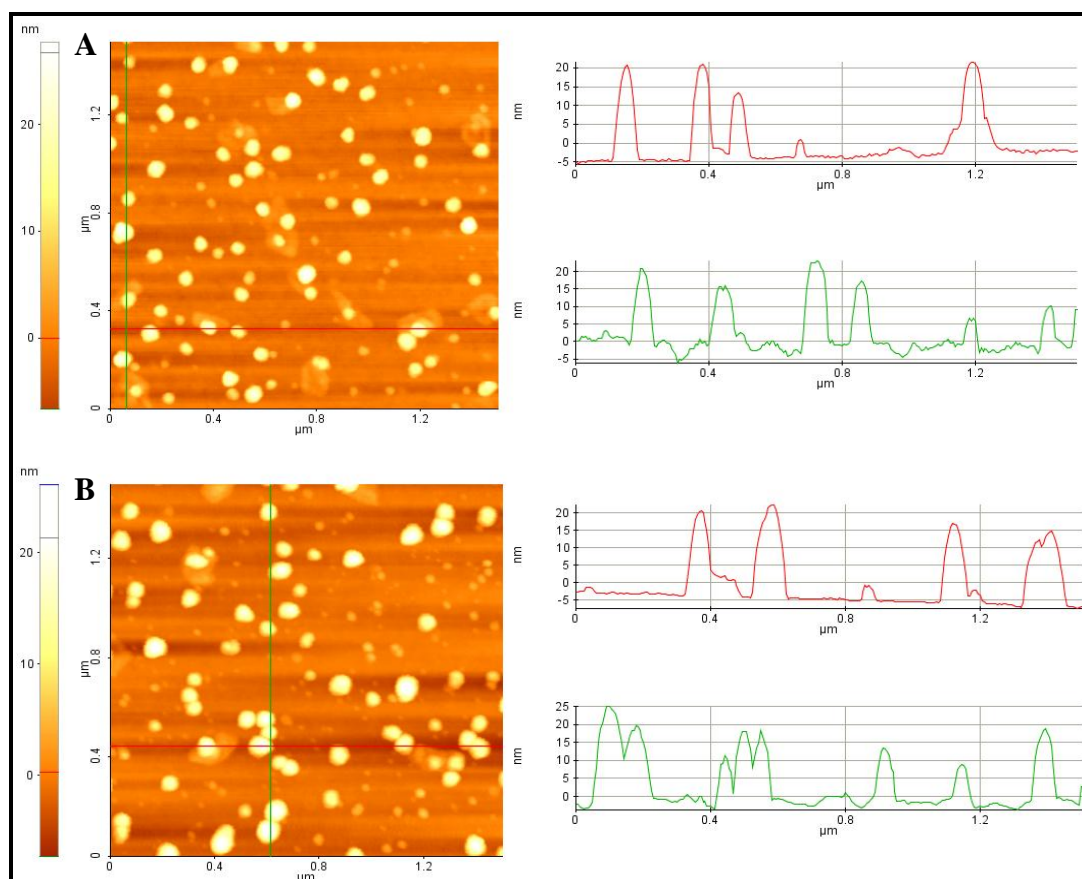


Figure 5.19. AFM image of round shaped aggregates formed by A. D5 ODN linker and B. D6 ODN linker

5.2.4. Constructing Nanorings with ODNs D3 and D4

The formation of nanoring structures with the sequences composed of a single base type is further investigated. The D3 and D4 sequences are composed of 20 base long Poly- T. These ODNs were covalently linked to SWCNTs and D8, 40 base pair long Poly A group was used as an ODN linker molecule as illustrated in Figure 5.20.

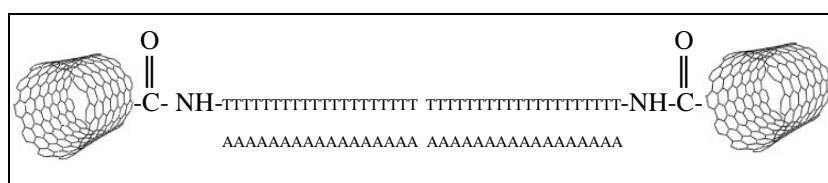


Figure 5.20. Representation of hybridization of ODNs D3 and D4 with ODN linker D8

Results indicate that these ODNs do not form ring structure and generate amorphous aggregates as shown in Figure 5.21. The reason for this is that since the ODN linker is complementary to ODNs on either end, the hybridization process is not controlled. For this reason, either D3 or D4 bound SWCNTs hybridize with themselves creating non-specific binding. Also these ODNs do not contain 10 Adenosine sequence that creates a distance between different SWCNTs from each other. Lack of this distance also contributes to the formation of amorphous aggregates. As seen in Figure 5.21A, there were various aggregates of SWCNTs, since ODN-SWCNTs were hybridizing in a random manner, unable to create a nanoring structure. Figure 5.21B, shows that aggregates nanotubes were still forming connections with each other in a few cases round structures resembling nanorings. However, looking at the overall image, these ring structures are irregular and has no resemblance to nanoring structures constructed with D1 and D2 ODNs. These results indicate that nanoring formation depends on strict control of ODNs and prevention of non-specific binding.

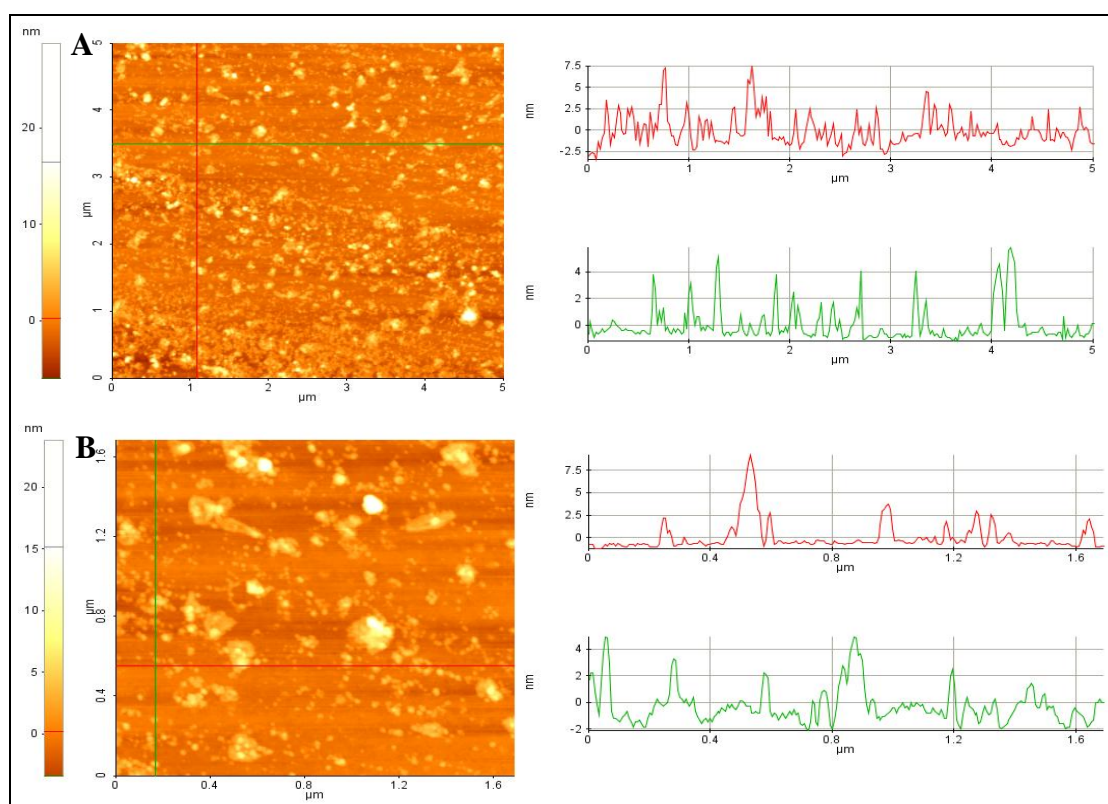


Figure 5.21. Non-shaped SWCNT aggregates formed by ODNs D3 and D4 with a A. General image and B. A close up

5.2.5. Effect of Sonication and Heat on the Stability of Nanorings

Since nanorings are constructed and held together by DNA hybridization, it is important to understand how they behave in the presence of external factors that destabilize their structure, and whether their shape is reversible after being subjected to the factors that targets DNA hybridization. Therefore, the suspension that includes the most successful nanoring forming components (ODNs D1 and D2 that were assembled in the presence of 5 mM ODN linker D7) were subjected to sonication and heating.

After sonicating nanorings for 5 minutes, a droplet of the suspension on a mica surface was placed and imaged with AFM. As seen on Figure 5.22, the nanorings structures were destroyed. Since the hybridized and assembled structure is destabilized, the ring form is lost. The AFM image shows long SWCNT bundles, but these bundles were not increased in thickness. The reason the nanoring structure is irreversible upon sonication is ODN linkers' non-covalent interactions and adsorption to SWCNT surfaces. This causes the bases of ODN linker to bind to SWCNT instead of the other ODNs to bring them together. As a result, nanorings are opened up and they are unable to fold back into their previous structures.

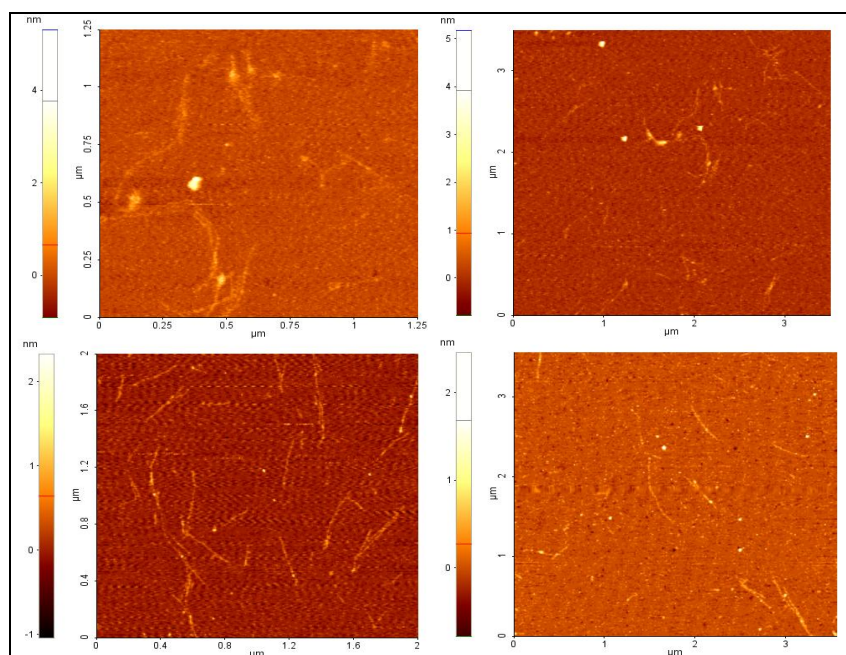


Figure 5.22. Opening up of nanorings after sonication

Another important external factor for nanoring assembly is heat since denaturation of dsDNA occurs at high temperatures. For this reason, nanorings are heated up to 95 °C and then cooled down to room temperature. However, even before the cooling down process occurs, when the temperature of the sample was 95 °C, nanorings in the sample dissociate and then form long rope shaped aggregates visible to the eye. This aggregate is not formed because of DNA hybridization since the sample was 95 °C. Its formation is related to the affinity of SWCNTs towards each other. Even though SWCNT molecules are carboxylated and they appear to be soluble in water, their affinity towards each other remains because carboxylation only occurs at the ends of SWCNTs, not all of the sidewalls. When DNA mediated structures are broken in these temperatures, SWCNTs tend to find each other to form aggregates. Since SWCNTs are DNA bound, formed aggregate don't precipitate, they can float in water because even though SWCNTs hide their hydrophobic parts by clustering together, they also have DNA bound hydrophilic parts that tend to associate with water. Since the aggregate is very big, it was observed in SEM instead of AFM. As shown in Figure 5.23. the aggregate has thick bundles and rope like structures that has a thickness of several μm .

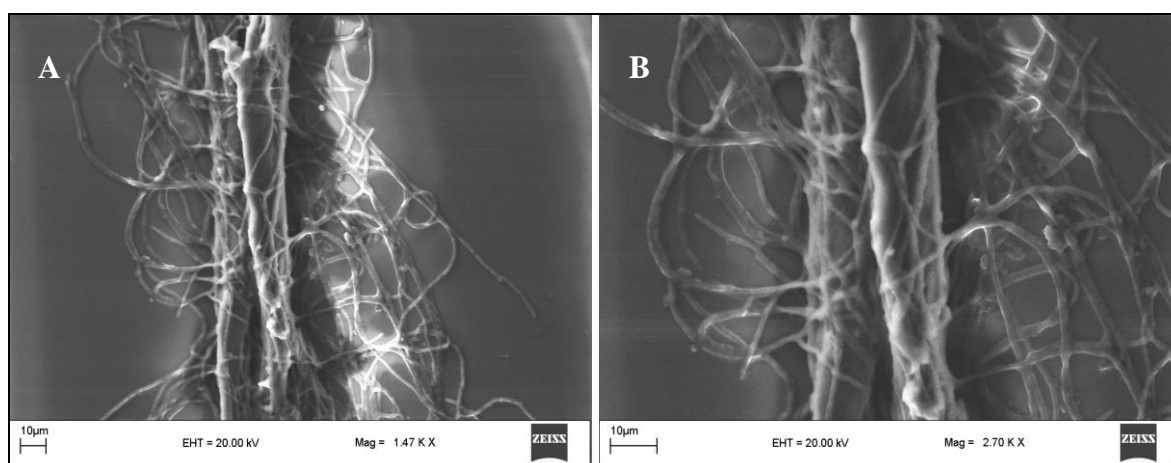


Figure 5.23. A. SEM image of aggregates composed of bundles and rope like structures formed after heating of nanorings and B. A close up image of the same structure

Overall, these results indicate that nanoring structures are not reversible upon sonication or heating because of the properties of SWCNTs and their interactions. When they are sonicated, ODN linkers bind to SWCNTs to make them more soluble and prevent them

from aggregation. Also sonication debundles SWCNTs and without free ODN linker molecules, they are unable to assemble into nanorings again. When they are heated, SWCNTs bundle together forming large aggregates, so they are unable to assemble into nanorings again.

6. CONCLUSION AND RECOMMENDATIONS

6.1. CONCLUSION

Carbon Nanotubes are one of the most promising nanomaterials but their tendency to form bundles makes them problematic for a wide variety of applications. Therefore, their dispersion and controlled self-assembly is essential for future applications. This thesis explored the use of DNA hybridization for the assembly of carbon nanotubes to construct higher structures. ODNs were designed to bring SWCNTs together in a controlled manner by creating an adjustable distance between them.

ODN linkers that connect these ODN-SWCNTs together contain spacer Adenosine molecules to give nanostructure flexibility so that it can fold into nanoring shape. By changing the concentration of ODN linker molecules that bind two SWCNTs together, nanoring structures were formed. Then, the factors that influenced nanoring formation were investigated. Since nanorings are formed due to deposition of SWCNTs onto surfaces, their formation differs between the rough hydrophilic glass and smoother mica surfaces, and they were unable to assemble on hydrophobic TEM grids, which prevented further characterization of nanorings to elucidate SWCNT orientation. Also, ODN linker concentration plays an essential role during nanoring formation since lower amounts of ODN linkers formed incomplete bending and interaction of SWCNTs and excessive amounts of ODN linker formed deformed nanoring structures since they adsorbed to the surface of SWCNTs and prevented the necessary aggregation nanorings require. ODNs consisting of single bases showed the importance of sequence specificity in the formation of nanorings. Also these ODNs did not contain 10 base pair long Adenosine molecules that create a distance between SWCNT and the hybridized part of ODN assisting the assembly of nanorings.. Non-specific interactions between ODN-SWCNTs and ODN linker also showed that the formation of nanorings depends on the specific DNA sequences without random hybridization. The effect of sonication and heat was shown to be disruptive to the nanoring structure and irreversible due to the interactions between SWCNT and DNA molecules.

In conclusion, nanorings were produced using DNA self-assembly. This thesis also showed that by changing the parameters of self-assembly, such as the ratio of hybridized DNA-SWCNT complexes or ODN linker concentration, these nanostructures assume different shapes, which can be investigated in future research on self-assembly. Also the factors outlined in this thesis provide a framework for further self-assembly research on SWCNTs .

6.2. RECOMMENDATIONS

In future work, using the building blocks that were outlined on this thesis, complex nanostructures based on nanorings can be designed. Using multistep approaches, several types of nanorings can be constructed and hybridized between each other to form complex networks using DNA hybridization. These nanorings can be used for the producing nanoelectronic devices and surfaces with different properties.

While this thesis outlines nanoring formation on glass and mica surfaces with changing ODN linker concentration, their assembly patterns in a suspension was not investigated. A research project in that direction would allow us to observe DNA-SWCNT dynamics in suspension, thus creating nanostructures that can be used for gene delivery. These nanorings can also be modified with sugar molecules or specific antibodies to target cancer cells. Since these structures are dissociated upon heating, non-invasive lasers can be used for controlled gene and drug delivery. Using this method, release of certain drugs and genes can be restricted to specific sites in the body, mostly for cancer research. For these reasons, it is essential to evaluate *in vitro* and *in vivo* toxicity of these nanorings. Because of the wide range of surface modifications available to researchers, it is also possible to PEGylate or the use of other polymers to introduce these structures to the body. This way, their toxicity issues would be addressed and they can be used for photothermal therapy, where SWCNTs are excited with 785 nm Near Infra Red laser and heat the cell they are inside, inducing apoptosis.

While this thesis describes only the binding of two different ODN-SWCNT complexes together, there are various nanostructures created with DNA self-assembly approach such as DNA tiles that can be hybridized with SWCNTs. These complex nanostructures provide various platforms to assemble SWCNTs into specific patterns, so in the future DNA

mediated SWCNT self-assembly can be applied to create more complex patterns using these structures.

7. REFERENCES

1. Reibold, M., P. Paufler, A. A. Levin, W. Kochmann, N. Patzke and D. C. Meyer, “Materials: Carbon nanotubes in an ancient Damascus sabre” , *Nature*, Vol. 444, No. 7117, pp. 286, 2006.
2. Feynman, R. P. , “There is plenty of room at the bottom” *Caltech Engineering and Science*, Vol. 23, No. 1, pp. 22-36, 1960.
3. Taniguchi, N. , “On the Basic Concept of Nanotechnology”, *Proc. of the Int. Conference on Production Engineering*, pp. 18–23, 1974.
4. Drexler, K. E. , “Engines of Creation: The Coming Era of Nanotechnology”, *New York Anchor*, 1986.
5. Meador, M. A., NASA Nanotechnology Roadmap, http://www.nasa.gov/pdf/501325main_TA10-Nanotech-DRAFT-Nov2010-A.pdf, [November 2010].
6. Schrödinger, E., “An Undulatory Theory of the Mechanics of Atoms and Molecules”, *Physical Review*, Vol. 28, No. 6, pp. 1049-1070, 1920.
7. Binnig, G., C. F. Quate, and Ch. Gerber., “Atomic Force Microscope”, *Physical Review Letters*, Vol. 56, No. 9, pp. 930-933, 1986.
8. Chapman, U., C. Hall, and J. M. Yorifanc Cirotjp., “Self assembly”, *Current Opinion in Colloid Interface Science*, Vol. 14, No. 2, pp. 61, 2007.
9. Zernike, F., “Overview of extreme ultraviolet lithography”, *Proceedings of the SPIE The International Society for Optical Engineering*, Vol. 2322, No. 3, pp. 430-433, 1994.

10. Tandon, U. S., “An overview of ion beam lithography for nanofabrication”, *Vacuum*, Vol. 43, No. 3, pp. 241-251, 1992.
11. Adams, T. M. and R. A Layton., “Chapter 3. Creating and transferring patterns—Photolithography”, *Introductory MEMS Fabrication and Applications*, Vol. 1, No. 3, pp. 65-94, 2010.
12. Cerrina, F., “X-Ray Lithography”, *Microelectronic Engineering*, Vol. 5, No. 3, pp. 6-16, 1996.
13. Kelly, R., “Electron Beam Lithography”, *Contemporary Physics*, Vol. 2, No. 3, pp. 457-462, 2008.
14. Tabeling, P., “Introduction to Microfluidics”, *Angewandte Chemie*, Vol. 118, No. 47, pp. 8039-8040, 2006.
15. Paul C., H. Li and Xiujun Li., “Microfluidic Lab-on-a-Chip”, *Technology*, 2008.
16. Sonntag, F, S. Schmieder, N. Danz, M. Mertig, N. Schilling, U. Klotzbach, and E. Beyer., “Novel lab-on-a-chip system for the label-free detection of DNA hybridization and protein-protein interaction by surface plasmon resonance (SPR)” , *Proceedings of SPIE*, Vol. 7365, pp. 1-9, 2009.
17. Hawtin, P., I. Hardern, R. Wittig, J. Mollenhauer, A. Poustka, R. Salowsky, T. Wulff, C. Rizzo, and B. Wilson., “Utility of lab-on-a-chip technology for high-throughput nucleic acid and protein analysis”, *Electrophoresis*, Vol. 26, No. 19, pp. 3674-3681, 2005.
18. Tasdemir, F., S. Zehir, E. Ozeren, J. H. Niazi, A. Qureshi, and S. S. Kallempudi., “A New Lab-on-Chip Transmitter for the Detection of Proteins Using RNA Aptamers”, *Spectrum*, pp. 489-492, 2010.

19. Kim, S., E. Hall, and R. N. Zare., "Microfluidics-based cell culture for single-cell analysis", *Biophysical Journal*, Vol. 650, 2007.
20. Gates, B. D., "New approaches to nanofabrication: Molding, printing, and other techniques", *Chemical Reviews*, Vol. 105, pp. 1171-1196, 2005.
21. Shimomura, M., and T. Sawadaishi., "Bottom-up strategy of materials fabrication: a new trend in nanotechnology of soft materials", *Current Opinion in Colloid Interface Science*, Vol. 6, No. 1, pp. 11-16, 2001.
22. Li, H., S. H. Park, J. H. Reif, T. H. LaBean, and H. Yan., "DNA-templated self-assembly of protein and nanoparticle linear arrays", *Journal of the American Chemical Society*, Vol. 126, No. 2, pp. 418-419, 2004.
23. Nuraje, N., K. Su, J. Samson, A. Haboosheh, R. I. Maccuspie, and H. D. A. Jul-Aug Matsui., "Self-assembly of Au nanoparticle-containing peptide nano-rings on surfaces", *Supramolecular Chemistry*, Vol. 18, No. 5, pp. 429-434, 2006.
24. Box, P. O., "SUMMiT V TM Five Level Surface Micromachining Technology I : Overview and Technology Description", *Energy*, pp. 1-27, 2005.
25. Yan, H., "Self-assemble symm finite DNA microarray nanoarray", *Journal of the American Chemical Society*, Vol. 127, pp. 17140, 2005.
26. Jain, P. K., and M. A. El-Sayed., "Plasmonic coupling in noble metal nanostructures", *Chemical Physics Letters*, Vol. 487, No. 4-6, pp. 153-164, 2010.
27. Praig, V. G, H. McIlwee, C. L. Schauer, R. Boukherroub, and S. Szunerits., "Localized surface plasmon resonance of gold nanoparticle-modified chitosan films for heavy-metal ions sensing", *Journal of Nanoscience and Nanotechnology*, Vol. 9, No. 1, pp. 350-357, 2009.

28. Cam, D., K. Keseroglu, M. Kahraman, F. Sahin, and M. Culha., “Multiplex identification of bacteria in bacterial mixtures with surface-enhanced Raman scattering”, *Journal of Raman Spectroscopy*, Vol. 41, No. 5 pp. 484-489, 2009.
29. Massich, M. D., D. A. Giljohann, A. L. Schmucker, P. C. Patel, and C. A. Mirkin, “Cellular response of polyvalent oligonucleotide-gold nanoparticle conjugates”, *ACS Nano*, Vol. 4, No. 10, pp. 5641-5646, 2010.
30. Grzelczak, M., J. Vermant, E. M. Furst and L. M. Liz-Marzan, “Directed self-assembly of nanoparticles”, *ACS Nano*, Vol. 4, No: 7, pp. 3591-3605, 2010.
31. Jain P. K., I. H. El-Sayed, and M. A. El-Sayed, “Au nanoparticles target cancer”, *Nano Today*, Vol. 2, pp. 18-29, 2007.
32. Duncan, B., C. Kim, and V. M. Rotello., “Gold nanoparticle platforms as drug and biomacromolecule delivery systems”, *Journal of Controlled Release*, Vol. 148, No. 1, pp. 122-127, 2010.
33. Prema, P. and R. Raju., “Fabrication and characterization of silver nanoparticle and its potential antibacterial activity”, *Biotechnology and Bioprocess Engineering*, Vol. 14, No. 6, pp. 842-847, 2010.
34. Tian, J., K. Kenneth, Y. Wong, C. M. Ho, C. N. Lok, W. Y. Yu, C. M. Che, J. F. Chiu, and P. K. H. Tam., “Topical delivery of silver nanoparticles promotes wound healing”, *Chemmedchem*, Vol. 2, No. 1, pp. 129-136, 2007.
35. Gao, J., G. Hongwei, and X. Bing, “Multifunctional Magnetic Nanoparticles : Design, Synthesis, and Biomedical Applications”, *Accounts of Chemical Research*, Vol. 42, No. 8, pp. 1097-1107, 2009.

36. Nash, M. A., Y. Paul, A. S. Hoffman, and P. S. Stayton., “Mixed stimuli-responsive magnetic and gold nanoparticle system for rapid purification, enrichment, and detection of biomarkers”, *Bioconjugate Chemistry*, Vol. 21, No. 12, pp. 2197-2204, 2010.
37. Byrne, S. J., S. A. Corr, Y. K. Gunko, J. M. Kelly, D. F. Brougham, and S. Ghosh. “Magnetic nanoparticle assemblies on denatured DNA show unusual magnetic relaxivity and potential applications for MRI”, *Chemical Communications*, No. 22 pp. 2560-2561, 2004.
38. Reed, M. A. “Quantum Dots”, *Physics World*, Vol. 268, No.1 pp.118-123, 1993.
39. Efros, A., M. Rosen, M. Kuno, M. Nirmal, Dj. Norris, and M. Bawendi, “Band-edge exciton in quantum dots of semiconductors with a degenerate valence band: Dark and bright exciton states”, *Physical review B Condensed matter*, Vol. 54, No. 7, pp. 4843-4856, 1996.
40. Ghasemi, Y., P. Peymani, and S. Afifi, “Quantum dot: magic nanoparticle for imaging, detection and targeting”, *Acta biomedica Atenei Parmensis*, Vol. 80, No. 2 pp. 156-165, 2009.
41. Xie, S., W. Li, Z. Pan, B. Chang, and L. Sun, “Mechanical and physical properties on carbon nanotube.”, *Journal of Physics and Chemistry of Solids*, Vol. 61, No. 7, pp. 1153-1158, 2000.
42. Nguyen, C. V., Q. Ye, and M. Meyyappan, “Carbon nanotube tips for scanning probe microscopy: fabrication and high aspect ratio nanometrology”, *Measurement Science and Technology*, Vol. 16, No. 11, pp. 2138-2146, 2005.
43. Gabay, T., M. Ben-David, I. Kalifa, R. Sorkin, Z. R. Abrams, E. Ben-Jacob, and Y. Hanein, “Electro-chemical and biological properties of carbon nanotube based multi-electrode arrays”, *Carbon Nanotubes*, Vol. 435, pp. 260-275, 2006.

44. Terrones M., A. G. S. Filho, and A.M. Rao, "Doped Carbon Nanotubes : Synthesis , Characterization and Applications", *Carbon Nanotubes*, Vol. 566, pp. 531-566, 2008.
45. Zhou, C., "Carbon Nanotube Nanoelectronics and Macroelectronics", *10th IEEE International Conference on SolidState and Integrated Circuit Technology*, pp. 1210., 2010.
46. Druzhinina, T. S., S. Hoepfner, and U. S. Schubert, "Microwave-assisted fabrication of carbon nanotube AFM tips", *Nano Letters*, Vol. 10, No. 10, pp. 4009-4012, 2010.
47. Bhirde, A. A., V. Patel, J. Gavard, G. Zhang, A. A. Sousa, A. Masedunskas, R. D. Leapman, R. Weigert, J. S. Gutkind, and J. F. Rusling, "Targeted killing of cancer cells in vivo and in vitro with EGF-directed carbon nanotube-based drug delivery", *ACS Nano*, Vol. 3, No. 2, pp. 307-316, 2009.
48. Kim, J., E. V. Shashkov, E. I. Galanzha, N. Kotagiri, and V. P. Zharov, "Photothermal antimicrobial nanotherapy and nanodiagnostics with self-assembling carbon nanotube clusters", *Lasers in Surgery and Medicine*, Vol. 39, No. 7, pp. 622-634, 2007.
49. Wohlstadter, J. N., J. L. Wilbur, G. B. Sigal, H. A. Biebuyck, M. A. Billadeau, L. Dong, A. B. Fischer, "Carbon Nanotube-Based Biosensor", *Advanced Materials*, Vol. 15, No. 14, pp. 1184-1187, 2003.
50. Iijima, S., "Helical microtubules of graphitic carbon", *Nature*, Vol. 354, No. 6348 pp. 56-58, 1991.
51. Avouris, P., "Carbon nanotube electronics", *Proceedings of the IEEE*, Vol. 9, No. 11 pp. 1772-1784, 2003.

52. Bekyarova, E., Y. Ni, E. B. Malarkey, V. Montana, J. L. McWilliams, R. C. Haddon, and V. Parpura, "Applications of Carbon Nanotubes in Biotechnology and Biomedicine", *Journal of Biomedical Nanotechnology*, Vol 1, No. 1, pp. 3-17, 2007.
53. Léonard, F., "The Physics of Carbon Nanotube Devices.", *Sensors*, pp. 300, 2009.
54. Peng, X., and S. S. Wong, "Functional Covalent Chemistry of Carbon Nanotube Surfaces", *Advanced Materials*, Vol. 21, No. 6, pp. 625-642, 2009.
55. Pampaloni, F., and E. L. Florin, "Microtubule architecture: inspiration for novel carbon nanotube-based biomimetic materials", *Trends in biotechnology*, Vol. 26, No. 6, pp. 302-310, 2008.
56. Ebbesen, T. W., "Carbon Nanotubes", *Annual Review of Materials Science* Vol. 24, No. 1, pp. 235-264, 1994.
57. Ajayan, P. M., "Nanotubes from Carbon", *Chemical Reviews*, Vol. 99, No. 7, pp. 1787-1800, 1999.
58. Iijima, S. and T. Ichihashi, "Single-shell carbon nanotubes of 1-nm diameter", *Nature*, Vol. 363, No. 6430, pp. 603-605, 1993.
59. Dresselhaus, M. S., G. Dresselhaus, and P. C. Eklund., "Science of Fullerenes and Carbon Nanotubes", *Science of Fullerenes and Carbon Nanotubes*, pp. 171, 1996.
60. Wang, N., Z. K. Tang, G. D. Li, and J. S. Chen, "Single-walled 4 Å carbon nanotube arrays", *Nature*, Vol. 408, No. 6808, pp. 50-51, 2000.
61. Journet, C., W. K. Maser, P. Bernier, and A. Loiseau, "Large-scale production of single-walled carbon nanotubes by the electric-arc technique", *Nature*, Vol. 388, pp. 20-22, 1997.

62. Rinzler, A. G., J. Liu, H. Dai, P. Nikolaev, C. B. Huffman, F. J. Rodríguez-Macías, P. J. Boul, “Large-scale purification of single-wall carbon nanotubes: process, product, and characterization”, *Applied Physics A Materials Science Processing*, Vol. 67, No. 1, pp. 29-37, 1998.
63. Cassell, A. M., J. A. Raymakers, J. Kong, and H. Dai, “Large Scale CVD Synthesis of Single-Walled Carbon Nanotubes”, *The Journal of Physical Chemistry B*, Vol. 103, No. 31, pp. 6484-6492, 1999.
64. Nikolaev, P., “Gas-phase catalytic growth of single-walled carbon nanotubes from carbon monoxide”, *Chemical Physics Letters*, Vol. 313, No. 1-2, pp. 91-97, 1997.
65. Su, M., “A scalable CVD method for the synthesis of single-walled carbon nanotubes with high catalyst productivity”, *Chemical Physics Letters*, Vol. 322, No. 5, pp. 321-326, 2000.
66. Reilly, R. M., “Carbon nanotubes: potential benefits and risks of nanotechnology in nuclear medicine”, *Journal of Nuclear Medicine*, Vol. 48, No. 7, pp. 1039-1042, 2007.
67. Fu, K., and Y. Sun, “Dispersion and solubilization of carbon nanotubes”, *Journal of Nanoscience and Nanotechnology*, Vol. 3, No. 5, pp. 351-364, 2003.
68. Webber, S. E., “Functionalization of Carbon Nanotubes”, *Anion Sensing*, Vol. 141, No. 1-2, pp. 193-237, 2003.
69. Yang, Y., H. Zou, B. Wu, Q. Li, J. Zhang, Z. Liu, X. Guo, and Z. Du, “Enrichment of Large-Diameter Single-Walled Carbon Nanotubes by Oxidative Acid Treatment” , *The Journal of Physical Chemistry B*, Vol. 106, No. 29, pp. 7160-7162, 2002.
70. Liu, J., A. G. Rinzler, H. Dai, J. H. Hafner, R. K. Bradley, P. J. Boul, A. Lu, “Fullerene Pipes”, *Science*, Vol. 280, No. 5367, pp. 1253-1256, 1998.

71. Huang, W., S. Taylor, K. Fu, Y. Lin, D. Zhang, T. W. Hanks, A. M. Rao, and Y. Sun, "Attaching Proteins to Carbon Nanotubes via Diimide-Activated Amidation", *Nano Letters*, Vol. 2, No. 4, pp. 311-314, 2002.
72. Abuilaiwi, F. A., T. Laoui, M. AlHarthi, and M. A. Atieh, "Modification and Functionalization of MWCNTs via Fischer Esterification", *Arabian Journal For Science And Engineering*, Vol. 35, No. 1, pp 37-48, 2010.
73. Zheng, M., A. Jagota, E. D. Semke, B. A. Diner, R. S. Mclean, S. R. Lustig, R. E. Richardson, and N. G. Tassi, "DNA-assisted dispersion and separation of carbon nanotubes", *Nature Materials*, Vol. 2, No. 5, pp. 338-342, 2003.
74. Besteman, K., J. Lee, F. G. M. Wiertz, H. A. Heering, and C. Dekker, "Enzyme-Coated Carbon Nanotubes as Single-Molecule Biosensors", *Nano Letters, Carbon Nanotubes* Vol. 3, No. 6, pp. 727-730, 2003.
75. "Atomic force microscopic study on DNA-wrapping for different diameter single-wall carbon nanotubes", *Diamond and Related Materials*, Vol. 17, No. 7-10, pp 1389-1393, 2008.
76. Wang Y., Z. Iqbal, and S.V. Malhotra, "Functionalization of carbon nanotubes with amines and enzymes", *Chemical Physics Letters*, Vol. 402, pp. 96-101, 2005.
77. Zheng, M., A. Jagota, E. D. Semke, B. A. Diner, R. S. McLean, S. R. Lustig, R. E. Richardson, and N. G. Tassi, "DNA-assisted dispersion and separation of carbon nanotubes", *Nature Materials*, Vol. 2, No. 5, pp. 338-342, 2003.
78. Dwyer, C., M. Guthold, M. Falvo, S. Washburn, R. Superfine, and D. Erie, "DNA-functionalized single-walled carbon nanotubes", *Nanotechnology*, Vol. 13, No. 5 pp. 601-604, 2002.

79. Jiang, K., L. S. Schadler, R. W. Siegel, X. Zhang, H. Zhang, and M. Terrones, "Protein immobilization on carbon nanotubes via a two-step process of diimide-activated amidation", *Journal of Materials Chemistry*, Vol. 14, No. 1, pp. 37, 2004.
80. Simmons, T. J., J. Bult, D. P. Hashim, R. J. Linhardt, and P. M. Ajayan, "Noncovalent functionalization as an alternative to oxidative acid treatment of single wall carbon nanotubes with applications for polymer composites", *ACS Nano* Vol. 3, No. 4, pp. 865-870, 2009.
81. Star, A., J. P. Gabriel, K. Bradley, and G. Grüner, "Electronic Detection of Specific Protein Binding Using Nanotube FET Devices", *Nano Letters*, Vol. 3, No. 4, pp. 459-463, 2003.
82. Britto, P. J., K. S. V. Santhanam, and P. M. Ajayan, "Carbon nanotube electrode for oxidation of dopamine", *Bioelectrochemistry and Bioenergetics*, Vol. 41, No. 1, 121-125, 1996.
83. Boussaad, S., N. J. Tao, R. Zhang, T. Hopson, and L. A. Nagahara, "In situ detection of cytochrome c adsorption with single walled carbon nanotube device", *Chemical Communications*, Vol. 14, No. 13, pp. 1502, 2003.
84. Wang, J., and M. Musameh, "Carbon nanotube/teflon composite electrochemical sensors and biosensors", *Analytical Chemistry*, Vol. 75, No. 9, pp. 2075-2086, 2003.
85. Wang, J., G. Liu, and M. R. Jan, "Ultrasensitive electrical biosensing of proteins and DNA: carbon-nanotube derived amplification of the recognition and transduction events", *Journal of the American Chemical Society*, Vol. 126, No. 10, pp. 3010-3011, 2004.
86. Service, R.F., "Nanomaterials Show Signs of Toxicity", *Science*, Vol. 300, No. 20, pp. 243-244, 2003.

87. Lam, C. W., J. T. James, R. McCluskey, S. Arepalli, and R. L. Hunter, "A review of carbon nanotube toxicity and assessment of potential occupational and environmental health risks", *Critical Reviews in Toxicology*, Vol. 36, No. 3, pp. 189-217, 2006.
88. Mattson, M. P., R. C. Haddon, and A. M. Rao, "Molecular functionalization of carbon nanotubes and use as substrates for neuronal growth", *Journal of Molecular Neuroscience*, Vol. 14, No. 3, pp. 175-182, 2000.
89. Hu, H., Y. Ni, V. Montana, R. C. Haddon, and V. Parpura, "Chemically Functionalized Carbon Nanotubes as Substrates for Neuronal Growth", *Nano Letters* Vol. 4, No. 3, pp. 507-511, 2004.
90. Prakash, S., and A. G. Kulamarva, "Recent advances in drug delivery: potential and limitations of carbon nanotubes", *Recent patents on drug delivery formulation*, Vol. 1, No. 3, pp. 214-221, 2007.
91. Gao, Y., and I. Kyratzis, "Covalent Immobilization of Proteins on Carbon Nanotubes", *Chemie*, Vol. 19, No. 10, pp. 206-213, 2008.
92. Tsang, S. C., J. J. Davis, M. L. H. Green, H. Allen, O. Hill, Y. C. Leung, and P. J. Sadler, "Immobilization Of Small Proteins In Carbon Nanotubes - High- Resolution Transmission Electron-Microscopy Study And Catalytic Activity", *Chemical Communications*, No. 17, pp. 1803-1804, 1995.
93. Gasparac, R., P. Kohli, M. O. Mota, L. Trofin, and C. R. Martin, "Template Synthesis of Nano Test Tubes", *Nano* Vol. 4, No. 3, pp. 513-516, 2004.
94. Wong, S. S., E. Joselevich, A. T. Woolley, C. L. Cheung, and C. M. Lieber, "Covalently functionalized nanotubes as nanometre-sized probes in chemistry and biology", *Nature*, Vol. 394, No. 6688, pp. 52-55, 1998.
95. Hafner, J. H., C. L. Cheung, and C. M. Lieber, "Growth of nanotubes for probe microscopy tips", *Nature*, Vol. 398, No. 6730, pp. 761-762, 1999.

96. Baclayon, M., G. J. L. Wuite, and W. H. Roos, "Imaging and manipulation of single viruses by atomic force microscopy", *Soft Matter*, Vol. 6, No. 21, pp. 5273, 2010.
97. Cerrina, F., "X-ray Lithography: Process and applications", *Synchrotron Radiation News*, Vol. 9, No. 3, pp. 6-16, 1996.
98. Ivey, P., R. McWilliam, A. Maiden, G. Williams, A. Purvis, and L. Seed, "Photolithography on Three Dimensional Substrates", *56th Electronic Components and Technology Conference*, pp. 283-288, 2006.
99. Perello, D., M. Kim, S. Jeong, B. Kang, D. Bae, Y. Lee, and M. Yun., "CNT-FET Schottky Barrier Devices Fabricated by E-beam Lithography", *Microscopy and microanalysis*, Vol.14, No. 2, pp. 410-411, 2008.
100. Häffner, M., A. Haug, R. T. Weitz, M. Fleischer, M. Burghard, H. Peisert, T. Chassé, and D. P. Kern, "E-beam lithography of catalyst patterns for carbon nanotube growth on insulating substrates", *Microelectronic Engineering*, Vol. 85, No. 5-6, pp. 768-773, 2008.
101. Mortini, B., "Photosensitive resists for optical lithography", *Comptes Rendus Physique* Vol. 7, No. 8, pp. 924-930, 2006.
102. Levenson, M. D. "Wavefront Engineering For Photolithography", *Physics Today*, No. 3, pp. 28-36, 1993.
103. Wang, T., M. Jonsson, E. Campbell, and J. Liu, "Development of Carbon Nanotube Bumps for Ultra Fine Pitch Flip Chip Interconnection", *1st Electronic Systemintegration Technology Conference*, No. 2, pp. 892-895, 2006.

104. Seeman, N. C., “The challenge of structural control on the nanoscale : bottom-up self-assembly of nucleic acids in 3D”, *International Journal of Nanotechnology*, Vol. 2, No. 4, pp. 348-370, 2005.
105. Binder, W. H., “Supramolecular assembly of nanoparticles at liquid-liquid interfaces”, *Angewandte Chemie International Edition*, Vol. 44, No. 33 pp. 5172-5175, 2005.
106. Matsui, J., K. Yamamoto, and T. Miyashita., “Assembly of untreated single-walled carbon nanotubes at a liquid–liquid interface”, *Carbon*, Vol. 47, No. 6, pp. 1444-1450, 2009.
107. Deegan, R., O. Bakajin, T. Dupont, G. Huber, S. Nagel, and T. Witten, “Contact line deposits in an evaporating drop”, *Physical Review E Statistical Physics Plasmas Fluids And Related Interdisciplinary Topics*, Vol. 62, No. 1, pp. 756-65, 2000.
108. Keseroğlu, K., and M. Culha, “Assembly of nanoparticles at the contact line of a drying droplet under the influence of a dipped tip”, *Journal of Colloid and Interface Science*, Vol. 360, No. 1, pp. 8-14, 2011.
109. Duggal, R., F. Hussain, and M. Pasquali, “Self-Assembly of Single-Walled Carbon Nanotubes into a Sheet by Drop Drying”, *Advanced Materials*, Vol. 18, No. 1 pp. 29-34, 2006.
110. Hong, S. W., W. Jeong, H. Ko, M. R. Kessler, V. V. Tsukruk, and Z. Lin, “Directed Self - Assembly of Gradient Concentric Carbon Nanotube Rings”, *Advanced Functional Materials*, Vol. 18, No. 14, pp.2114-2122, 2008.
111. Hamad-Schifferli, K., J. J. Schwartz, A. T. Santos, S. Zhang, and J. M. Jacobson, “Remote electronic control of DNA hybridization through inductive coupling to an attached metal nanocrystal antenna”, *Nature*, Vol. 415, No. 6868, pp. 152-155, 2002.

112. Chworos, A., I. Severcan, A. Y. Koyfman, P. Weinkam, E. Oroudjev, H. G. Hansma, and L. Jaeger, "Building programmable jigsaw puzzles with RNA", *Science*, Vol 306, No. 5704, pp. 2068-2072, 2004.
113. Vauthey, S., S. Santoso, H. Gong, N. Watson, and S. Zhang, "Molecular self-assembly of surfactant-like peptides to form nanotubes and nanovesicles", *Proceedings of the National Academy of Sciences of the United States of America*, Vol. 99, No. 8, pp. 5355-5360, 2002.
114. Lim, Y. B., S. Park, E. Lee, H. Jeong, J. Ryu, M. S. Lee, and M. Lee, "Glycoconjugate nanoribbons from the self-assembly of carbohydrate-peptide block molecules for controllable bacterial cell cluster formation", *Biomacromolecules* Vol. 8, No. 5, pp. 1404-1408, 2007.
115. Tan, Y. C., A. Q. Shen, Y. Li, E. Elson, and L. Ma, "Engineering lipid tubules using nano-sized building blocks: the combinatorial self-assembly of vesicles", *Lab on a Chip*, Vol. 8, No. 2, pp. 339-345, 2008.
116. Hogberg, B., J. Helmersson, S. Holm, and H. Olin, "Study of DNA coated nanoparticles as possible programmable self-assembly building blocks", *Applied Surface Science*, Vol. 252, No. 15, pp. 5538-5541, 2006.
117. Mucic, R. C., J. J. Storhoff, C. A. Mirkin, and R. L. Letsinger, "DNA-Directed Synthesis of Binary Nanoparticle Network Materials", *Journal of the American Chemical Society*, Vol. 120, No. 48, pp. 12674-12675, 1998.
118. Glotzer, S. C., and J. A. Anderson, "Nanoparticle assembly: made to order", *Nature Materials*, Vol. 9, No. 11, pp. 885-887, 2010.
119. Lin, C., Y. Liu, S. Rinker, and H. Yan, "DNA tile based self-assembly: building complex nanoarchitectures", *Chemphyschem A European Journal Of Chemical Physics And Physical Chemistry*, Vol. 7, No. 8, pp. 1641-1647, 2006.

120. Feng, L., S. H. Park, J. H. Reif, and H. Yan, "A two-state DNA lattice switched by DNA nanoactuator", *Angewandte Chemie International Edition*, Vol. 42, No. 36, pp. 4342-4346, 2003.
121. Zhang, J., Y. Liu, Y. Ke, and H. Yan, "Periodic square-like gold nanoparticle arrays templated by self-assembled 2D DNA Nanogrids on a surface", *Nano Letters*, Vol. 6, No. 2, pp. 248-251, 2006.
122. Rothmund, P. W. K., "Design of DNA origami", *International Conference on ComputerAided Design*, pp. 471-478, 2005.
123. He, Y., T. Ye, M. Su, C. Zhang, A. E. Ribbe, W. Jiang, and C. Mao, "Hierarchical self-assembly of DNA into symmetric supramolecular polyhedra", *Nature*, Vol. 452, No. 7184, pp. 198-201, 2008.
124. Numajiri K., T. Yamazaki, M. Kimura, A. Kuzuya, and M. Komiyama, "Discrete and active enzyme nanoarrays on DNA origami scaffolds purified by affinity tag separation", *Journal of the American Chemical Society*, Vol. 132, pp. 9937-9939, 2010.
125. Sharma, J., R. Chhabra, A. Cheng, J. Brownell, Y. Liu, and H. Yan, "Control of self-assembly of DNA tubules through integration of gold nanoparticles", *Science*, Vol. 323, No. 5910, pp. 112-116, 2009.
126. Becerril, H. A., and A. T. Woolley, "DNA-templated nanofabrication", *Chemical Society Reviews*, Vol. 38, No. 2, pp. 329-337, 2009.
127. Andersen, E. S., M. Dong, M. M. Nielsen, K. Jahn, R. Subramani, W. Mamdouh, M. M. Golas, "Self-assembly of a nanoscale DNA box with a controllable lid", *Nature* Vol. 459, No. 7243, pp. 73-6, 2009.

128. Maune, H. T., S. Han, R. D. Barish, M. Bockrath, W. A. Goddard, P. W. K. Rothmund, and E. Winfree, "Self-assembly of carbon nanotubes into two-dimensional geometries using DNA origami templates", *Nature Nanotechnology*, Vol 5, No. 1, pp. 61-66, 2010.
129. Singh, P., F. M. Toma, J. Kumar, V. Venkatesh, J. Raya, M. Prato, S. Verma, and A. Bianco, "Carbon nanotube-nucleobase hybrids: nanorings from uracil-modified single-walled carbon nanotubes", *Chemistry*, Vol. 17, No. 24, pp. 6772-6780, 2011.
130. Movasaghi Z., S. Rehman, and I. U. Rehman, "Fourier Transform Infrared (FTIR) Spectroscopy of Biological Tissues", *Applied Spectroscopy Reviews*, Vol. 43, pp. 134-179, 2008.
131. Giordani, S., S. D. Bergin, V. Nicolosi, S. Lebedkin, M. M. Kappes, W. J. Blau, and J. N. Coleman, "Debundling of single-walled nanotubes by dilution: observation of large populations of individual nanotubes in amide solvent dispersions", *The Journal of Physical Chemistry B*, Vol. 110, No. 32, pp. 15708-15718, 2006.